

1962

# Further investigation into the shear strength of prestressed concrete beams without web reinforcement, (Progress Report No. 22), Lehigh University, January 1962

F. McClarnon

M. Wakabayashi

C. E. Ekberg Jr.

Follow this and additional works at: <http://preserve.lehigh.edu/engr-civil-environmental-fritz-lab-reports>

---

## Recommended Citation

McClarnon, F.; Wakabayashi, M.; and Ekberg, C. E. Jr., "Further investigation into the shear strength of prestressed concrete beams without web reinforcement, (Progress Report No. 22), Lehigh University, January 1962" (1962). *Fritz Laboratory Reports*. Paper 1524. <http://preserve.lehigh.edu/engr-civil-environmental-fritz-lab-reports/1524>

This Technical Report is brought to you for free and open access by the Civil and Environmental Engineering at Lehigh Preserve. It has been accepted for inclusion in Fritz Laboratory Reports by an authorized administrator of Lehigh Preserve. For more information, please contact [preserve@lehigh.edu](mailto:preserve@lehigh.edu).

PRESTRESSED CONCRETE BRIDGE MEMBERS

Progress Report 22

FURTHER INVESTIGATION INTO THE  
SHEAR STRENGTH OF PRESTRESSED CONCRETE BEAMS  
WITHOUT WEB REINFORCEMENT

Francis M. McClarnon

Minoru Wakabayashi

Carl E. Ekberg, Jr.

Lehigh University  
Bethlehem, Pennsylvania

Fritz Laboratory Report No. 223.22

January, 1962

## TABLE OF CONTENTS

	Page
INTRODUCTION	1
Object and Scope	1
Outline of Tests	2
Notation	2
DETAILS OF TEST SPECIMENS	3
Materials	3
Cement	3
Aggregates	3
Concrete	3
Reinforcing	5
Description of the Specimens	5
Prestressed Beams	6
Non-Prestressed Beams	7
Casting and Curing	8
Prestress Losses	9
LOADING APPARATUS, INSTRUMENTATION AND OUTLINE OF TEST PROCEDURE	10
Loading Apparatus	10
Instrumentation	10
Ames Dial Gages	10
Photographs	11

	Page
Outline of Typical Test Procedure	11
Preliminary	11
Test Procedure	12
<b>BEHAVIOR OF TEST SPECIMENS AND TEST RESULTS</b>	<b>14</b>
Cracking Characteristics	14
Flexural Cracks	14
Inclined Cracks	15
Classification of Failures	16
Load-Deflection Relations	17
Typical Photographs of a Beam During Testing	18
Photographs of Beams After Testing	18
<b>STRENGTH OF PRESTRESSED AND REINFORCED CONCRETE BEAMS WITHOUT WEB REINFORCEMENT</b>	<b>19</b>
Modes of Failure	19
Flexural Failure	19
Shear Compression Failure	20
Diagonal Tension Failure	22
Bond Failure	23
Conclusions	24
<b>REVISION OF SHEAR COMPRESSION THEORY</b>	<b>25</b>
Basic Concept of the Shear Compression Theory	25
Development of the Shear Compression Theory Equations	25

	Page
New Evaluation of Bond Parameter	29
Compatibility Condition Reviewed	31
Discussion of Limiting Stress	32
<b>COMPARISON OF REVISED THEORY WITH TEST RESULTS</b>	<b>34</b>
<b>DISCUSSION OF CONDITIONS AFFECTING ULTIMATE STRENGTH</b>	<b>36</b>
Length of Overhang	36
General	36
Effect of Type of Reinforcing	37
Effect of Prestress	40
Effect of Shear Span	41
Conclusions	42
Effect of Existing Inclined Cracks	42
General	42
Results of Tests	43
Conclusions	44
Height of Load Point	45
General	45
Results of Tests	45
Conclusions	47
<b>SUMMARY</b>	<b>49</b>

	Page
ACKNOWLEDGEMENTS	54
TABLES AND FIGURES	56
REFERENCES	99

## INTRODUCTION

### Object and Scope

The tests described in this report, on beams of prestressed and conventionally reinforced design, were undertaken to determine the effect of length of overhang at the reaction, existing inclined cracks, and height of load point on the ultimate strength of prestressed beams without web reinforcement. In addition, these tests were used to modify the shear compression theory proposed in Progress Report 17 and 17A<sup>(1,2)\*</sup>.

This shear compression theory provides a procedure to compute the ultimate strength of prestressed concrete beams without web reinforcement subjected to combined bending moment and shear. When it was originally applied to beams tested at Lehigh in 1958<sup>(3)</sup>, some lack of agreement between theoretical predictions of ultimate strength and corresponding experimental values was apparent. This fact necessitated a review and revision of the theory so that closer agreement with test data could be obtained. In addition it was necessary to determine the limitations on the

---

\* Raised numerals in parentheses correspond to works listed in the references.

practical application of the theory.

### Outline of Tests

The results of twenty-eight beam tests, of both rectangular and I-shaped cross section, are presented in this report. Sixteen of these tests, used to determine the effect of length of overhang and the effect of existing inclined cracks, were designated as Series C, and are outlined in Table I. All beams in Series C were of rectangular cross section.

The remaining twelve beam tests were conducted to evaluate the effect of manner of loading. These tests were designated as Series D, and are outlined in Table II.

### Notation

The notation generally used in this report is consistent with that recommended by the A.C.I. - A.S.C.E. Joint Committee 323.<sup>(4)</sup> Several additional terms are explained wherever they appear in the text.



## DETAILS OF TEST SPECIMENS

### Materials

#### Cement

Type III Portland Cement, manufactured by the Lone Star Cement Company, was used in all beams. Deliveries were made at approximately two-week intervals, during the period when beams were made, so as to avoid prolonged storage of cement in the laboratory.

#### Aggregates

The coarse aggregate was crushed limestone having a maximum size of 1 in., and a gradation curve as shown in Fig. 1. The fine aggregate consisted of Lehigh River sand with a fineness modulus of 3.50, and a gradation as shown in Fig. 1.

#### Concrete

The concrete was designed to have a 28-day strength of 5500 psi and a slump of 2-1/2 in.

The proportions of the mix by weight were:

Cement	1.00
Coarse Aggregate (saturated surface dry)	3.27
Fine Aggregate (saturated surface dry)	3.27
Water	0.62

Properties of the concrete were determined from 6 x 12 in. cylinders and 6 x 6 x 36 in. modulus of rupture beams poured and tested the same day as their corresponding beam. The cylinders were capped with carbo-vitrobond on the top and bottom surfaces. The average cylinder strength for each beam is listed in Table III.

The modulus of rupture beams were loaded at the third points on a 30 in. span. A comparison of modulus of rupture strength with the compressive strength is shown in Fig. 2. The average modulus of rupture strength of all specimens tested was 660 psi.

The stress-strain characteristics of two concrete cylinders were determined. In both an average strain was measured by means of two diametrically opposite SR-4 electrical resistance gages (Type A-9) connected in series. Fig. 3 shows the non-dimensionalized stress-strain curves, which practically coincide, and which are assumed to be

indicative of the concrete in every beam.

### Reinforcing

The prestressed beams were of bonded pretensioned construction. In each case the tendons were high-strength stress-relieved 7/16 in. diam. strands and the stress-strain relationship for this steel is shown in Fig. 4.

Four of the beams in Series C were reinforced with No. 6 deformed reinforcing bars with an average yield strength of 32,900 psi.

### Description of the Specimens

Twenty-two beams with rectangular cross sections and six beams with I-shaped sections were made and tested. All beams had nominal out-to-out dimensions of 6 x 12 in., and the lengths varied from 5 ft.-11 in. to 11 ft.-6 in. Span lengths, and actual cross section dimensions measured in the region of failure are given in Table IV. Fig. 5 shows the details of the cross sections including the location of longitudinal reinforcement.

All but four of the beams shown in Table III were longitudinally reinforced with 7/16 in. diam. 7-wire

pretensioning strands. Those four (C13, C14, C15, C16) were reinforced with No. 6 deformed bars. All but three beams (D4, D5, D6) had a group of three stirrups placed at the supports. The stirrups consisted of No. 3 deformed bars bent and positioned as shown in Fig. 6. In these three beams (D4, D5, D6), the stirrups were inadvertently placed six inches inward toward the load points. Since the inclined crack in these tests did not cross any portion of a vertical bar, the effect of the misplaced stirrups was considered negligible. Therefore all beams were regarded as being without web reinforcement in the shear span.

#### Prestressed Beams (C5 through C12, D1 through D12)

Fourteen rectangular beams and six I-beams were prestressed with each beam having four 7/16 in. diam. strands. Initial as well as effective prestress values are given in Table III. Variation of tension between strands in a single beam was held within five percent. As observed in Table III the effective prestress in the rectangular beams varied from 46,200 psi to 55,000 psi, and the corresponding stress in the I-beams varied from 39,500 psi to 51,100 psi. The low prestress was used to reduce the resistance of the

beams to inclined cracking. Four strands were used in order to achieve a high ultimate strength.

The beams in Series D were cast with monolithic stubs designed to permit three different modes of load application. The load was transferred to the beam as follows:

Beams D1, D4, D7, D10 - Directly on top

Beams D2, D5, D8, D11 - On full stubs

Beams D3, D6, D9, D12 - On half stubs.

The mode of loading is shown in Table II. Details of the stubs are given in Fig. 7.

#### Non-Prestressed Beams (C1 through C4, C13 through C16)

Two groups, each of four non-prestressed beams, were tested. Beams C1 through C4 were reinforced with 7/16 in. diam. strand; Beams C13 through C16 were reinforced with No. 6 deformed bars. The prestress shown in Table III for Beams C1 through C4 were used to eliminate sag of the strands within each beam. The negative steel stresses for Beams C13 through C16 indicates that the reinforcement, due to shrinkage, underwent a small compression.

## Casting and Curing

The formwork consisted of pairs of steel channels 12 ft. long and 12 in. deep bolted to a plywood base with flanges facing outward. End sections consisted of steel channels for the beams with strand reinforcement and plywood for the remaining beams. Forms were placed so that three or four beams could be cast end to end in a row. Fig. 8 shows a photograph of the casting bed. The deformed bars were held at the proper elevation by bar chairs and tie wires. I-sections were formed by fastening timber blocks to the webs of the side channels providing the reduced section.

The concrete was mixed in six cu. ft. batches for approximately five minutes. The mixer used was a Lancaster Counter Current Batch Mixer, Model EB4. Two-wheeled buggies were used to transport the concrete to the forms where it was shoveled, vibrated and/or rodded into place. Concrete for three 6 x 12 in. control cylinders and one 6 x 6 x 36 in. modulus of rupture beam was taken from each batch concurrent with placement in the forms.

The curing operation consisted of wrapping the beams

in wet burlap and keeping them under moisture-proof plastic for four days, after which the side forms were removed. This was followed by air drying for one day to allow placement of Whittemore targets on the side of the beam. After the adhesive for the targets had dried (one additional day), the prestressing jacks were gradually released and the strands were cut with an acetylene torch. Curing was then resumed by covering with wet burlap. The beams were cured for eight weeks, after which the beams were air dried until the day of testing.

#### Prestress Losses

Elastic losses and losses due to creep plus shrinkage were estimated from strain measurements made on both sides of the beams at mid-span. The strain measurements were obtained with a Whittemore extensometer having a 10 in. gage length. The gage points consisted of aluminum plates approximately  $1/4 \times 1/4 \times 1/32$  in. cemented at various levels to both sides of the beam. Values of the total tensile stress in the steel before release, immediately after release, and at the time of test are given in Table III. These stresses were calculated on the basis that the change in strain on the surface of the concrete at the level of the steel is the same as the change in strain in the steel.

## LOADING APPARATUS, INSTRUMENTATION AND OUTLINE OF TEST PROCEDURE

### Loading Apparatus

The testing set-up is shown in detail in Fig. 9, and a photograph of a test underway is shown in Fig. 10. Test loads were applied with two 22-kip capacity Amsler jacks which were bolted to a steel frame. Jack loads were measured by a pendulum dynamometer.

### Instrumentation

Instrumentation consisted of Ames dial gages used to measure vertical deflections and SR-4 electrical resistance gages used to measure concrete strains, in addition to the Whittemore targets described in the previous section. Photographs were taken of some of the beams during testing in order to study crack patterns. No strain gages were placed on any of the principal reinforcing steel in the prestressed or conventionally reinforced beams.

#### Ames Dial Gages

A frame constructed from perforated aluminum members was set on knife-edge supports resting on the top surface



of the concrete beam. Ames dials were mounted to the frame and were located so as to measure the beam deflection at the center line, at a quarterpoint, and usually at the end extremities of the beam.

In every beam the strands or reinforcing bars projected outside the end faces. To detect relative slip, an Ames dial was bolted to one of these projecting tendons at each end of the beam. The dials were read at each test load increment.

#### Photographs

In the later stages of loading, photographs were taken of several beams before and after diagonal cracking. These were useful in ascertaining the accuracy of the compatibility condition. Every beam was photographed after failure.

### Outline of Typical Test Procedure

#### Preliminary

Immediately following placement of the beam in the testing position, Whittemore gage readings were taken to determine the final value of creep and shrinkage losses.

Also, the beams were whitewashed to facilitate observation of crack patterns.

### Test Procedure

The beams were loaded to failure in from fifteen to twenty increments. At each increment of load, all deflection and strain measurements were taken and the progress of the crack pattern was marked directly on the beam. Deflection readings were taken four or five minutes after each load increment was applied. The strain readings were usually begun just after the load increment was reached. At higher loads, a second series of strain readings was taken at the same load increment. Numerals were stenciled on each beam to indicate extension of cracks at a corresponding load in kips on each jack.

The rate of loading was usually two kips per minute, but in the later stages of loading this depended primarily on the development of the cracks. All but two beams were loaded directly to failure. These two, C6 and C10, were loaded until inclined cracks formed, then completely unloaded so that the jacks could be moved to increase the shear spans. Finally, with increased shear spans, these

beams were loaded to failure. The time required to test one beam varied from two and one-half to five hours.

## BEHAVIOR OF TEST SPECIMENS AND TEST RESULTS

This section describes the behavior of the test beams under applied loads up to and including the ultimate load. The cracking and ultimate loads, the cause of final failure, the load-deflection relations, photographs of a beam during testing, and the photographs of all beams after testing are given.

### Cracking Characteristics

Flexural and inclined cracks were the two types of cracking identified during the course of the testing. The nature of each of these types will be described in the following paragraphs.

#### Flexural Cracks

The load that causes the first vertical crack to form is called the flexural cracking load and is listed in Table V as  $V_{fc}$  for each beam. A flexural crack is caused by the tensile stresses induced by bending moment. In these tests when a flexural crack formed, it was of hair-line width. The crack was detected by a very close visual inspection of the beam. This cracking caused a

change in the shape of the load deflection curve. Before cracking the load deflection curve was linear, while after cracking the load deflection curve was somewhat linear, but the slope of the curve was decreased substantially. Flexural cracks were usually the first to appear; however in some of the I-beams the inclined cracks appeared first.

### Inclined Cracks

The load that causes the first inclined crack to develop is called the inclined cracking load and is denoted in Table V by the symbol  $V_{ic}$ . An inclined crack is a fully developed non-vertical crack that is caused by the combined effect of shear and bending moment.

The inclined cracking load is important because it marks a distinct change in the behavior of the beam. The member had previously been resisting loads by beam action, while after formation of an inclined crack the load is resisted by quasi-arch action. Furthermore, a beam without web reinforcement cannot be reliably loaded beyond inclined cracking; that is, a beam with such cracks is dangerous and unstable and has reached its practical ultimate load.

In rectangular beams there are two types of inclined cracks as illustrated in Fig. 11. One is the diagonal tension crack which may occur in a region previously uncracked or above a flexure crack. See Fig. 11-b. The second type occurs as the extension of a flexural crack slightly outside one or both load points and will be called a flexure-shear crack. See Figs. 11-c and 11-d.

The diagonal tension crack is initiated suddenly, often developing while the load is being held constant on the beam. This crack starts near the neutral axis of the beam, and its development is rapid. The diagonal tension crack shall be called an inclined crack as soon as it forms. An example of the development of this type of crack is shown in Fig. 12.

The flexure-shear crack is a flexural crack that becomes inclined and extends with increasing load slowly toward the load point. It is not considered fully developed until from the higher portion of the crack a new branch forms and progresses rapidly downward at an inclined angle.

#### Classification of Failures

The ultimate load resisted by each beam is listed in

Table V as  $V_u$ . This table also includes the particular mode of failure for each beam; F indicates flexural failure, S(SC) indicates shear failure in shear compression, S(DT) indicates shear failure in diagonal tension, and B indicates a bond failure. A discussion of each mode of failure is included in subsequent paragraphs.

#### Load-Deflection Relations

Deflections were measured by dial gages at three points for each beam, as shown in Fig. 9. Figures 13 through 20, inclusive, show the relationships between load and mid-span deflection grouped, as discussed in later sections of the report, to correspond with the purpose of testing. In the case of shear failures these curves are valuable in judging the relative strengths of similar beams.

Two interesting facts relative to the behavior of the beams are brought out by an examination of the load-deflection relationships in Figs. 13 and 14. First of all, the beams which were reinforced with unprestressed strands were consistently less rigid than the corresponding prestressed or conventionally reinforced beams. Secondly,

it is clear that the prestressed beams performed better, in every instance, in the range of load before cracking. After cracking the load-deflection relationships for the prestressed beams approaches coincidence with the corresponding conventionally reinforced beam.

#### Typical Photographs of a Beam During Testing

Photographs of Beam C8 taken during the testing operation are shown in Fig. 12. These illustrate the development of the inclined crack as the load increases and will be further discussed in the following section.

#### Photographs of Beams After Testing

Figures 21 through 31, inclusive, are photographs taken of each beam after testing. The photographs are arranged to correspond with the purpose of testing. Further discussion occurs later in the report.



STRENGTH OF PRESTRESSED AND REINFORCED CONCRETE  
BEAMS WITHOUT WEB REINFORCEMENT

Modes of Failure

There are four internal stress elements which can combine to cause failure in a beam, namely: bending moment, axial force, shear force, and torsion. This report considers only the effect of bending moment and shear forces. As previously indicated, failures in this series of tests were classified as follows: flexural, shear compression, diagonal tension, and bond.

Flexural Failure

Flexural failures may result in both under-reinforced and over-reinforced beams. In an under-reinforced beam, failure occurs after yielding of the steel, while in an over-reinforced beam, failure occurs before the stress in the steel reaches the yield level. In both cases, the failure mechanism is characterized by crushing of the concrete in the compression zone. The flexural failure phenomenon is basically the same for both rectangular and I-sections.

### Shear Compression Failure

Shear compression failure is due to the combined effect of flexural and shear forces. The development of a flexure-shear crack that may lead to a shear compression failure has been described in the previous section. Once such a crack has developed, it produces two effects on the beam being tested which combine to cause destruction of the beam. First, the flexure-shear crack produces a concentrated angular rotation in the beam, which locally increases stresses and tends to induce a premature moment failure. Second, the beam resists the applied external load by quasi-arch action. When the flexure-shear crack has developed fully to the point of being an inclined crack, the quasi-arch may not be a stable structure, and strength available after this crack has formed is not reliable.

Concerning the first effect, the concrete at the top of the flexure-shear crack is subjected to high normal and shear forces. As the applied load increases these forces increase, and the inclined crack penetrates further into the "compression zone". This decreases the amount of concrete available to resist the normal and shear forces.

As this concrete area takes larger and larger forces, the beam tends to redistribute the applied load by transferring some of the shear through the longitudinal reinforcement. This causes the crack to form another branch, which initiates at a high position on the crack and progresses rapidly downward at an angle of approximately  $45^\circ$  as indicated in Fig. 11. When this happens, the second effect is imposed on the beam. The beam is resisting the external loads by beam action and quasi-arch action. This development of the crack tends to make the beam structure an unstable one, depending on the particular location of the crack and the load or loads. The load which causes this development of the flexure-shear crack is called the inclined cracking load; it must be assumed that this is the ultimate load in a beam without web reinforcement, since the beam cannot reliably sustain greater loads. However, it is the combined effect of the bending and concentrated angular rotation, plus the possibly unstable quasi-arch action which causes final destruction. The maximum load is reached when the concrete at the top of the inclined crack is crushed or otherwise cannot be maintained in equilibrium.

After a flexure-shear crack forms, its progress is restricted by the presence of the load points when the

beam is loaded on top. If the beam is not loaded on top, or if the loads are not stationary, shear compression failure will probably not occur.

### Diagonal Tension Failure

Diagonal tension failure is a shear failure due to the combined effect of flexural and shear stresses. It occurs when a diagonal tension crack (an inclined crack) appears. The diagonal tension crack may occur in a region previously uncracked or above a flexural crack. From the starting point, the crack progresses rapidly toward the load point and away from it. The diagonal tension crack has a smaller angle of inclination than a flexure-shear crack. However, it is easier to differentiate between flexure-shear and diagonal tension cracks on the basis of beam behavior. When a flexure-shear crack develops fully and becomes an inclined crack, the resulting failure is usually a gradual, non-brittle type. A diagonal tension crack, however, may propagate without any substantial increase in load. After the diagonal tension crack has appeared, the stability of the beam is uncertain.

In non-rectangular beams with thin webs, crack formation is sudden. The presence of diagonal tension cracks

alters the behavior of the beam immediately. Sozen and others have developed an analysis of the strength and modes of failure for I-beams<sup>(5)</sup>. The six I-beams tested in Series D can be classified by means of this analysis. Four of these beams failed in diagonal tension by web crushing, and two by separation of the tension flange from the web. The beams that failed by web crushing were Beam D10 having an 18 in. shear span and loaded on the top, and Beams D7, D8, and D9 with 30 in. shear spans and loaded on top, on full stubs, and on half stubs, respectively. The beams that failed due to a splitting action near the junction between the lower flange and the web were Beams D11 and D12, having full-stub and half-stub loading, respectively.

#### Bond Failure

Two beams, C4 and C12, failed because there was insufficient distance, between the end of the beam and the point where the inclined crack crossed the longitudinal strand reinforcement, to develop the force in the strand needed to lead to either a shear compression or flexural failure. As a result, strand slip occurred, and this was termed bond failure.

Conclusions

If one categorizes diagonal tension failure and shear compression failure under the heading of shear failure, and disregards bond failure as due to poor dimensional proportioning, there are only two modes of beam failure, namely shear failure and flexure failure. Diagonal tension and shear compression failures are both caused by the formation of an inclined crack. As previously discussed, the inclined cracking load should be considered the ultimate load in beams without web reinforcement.

## REVISION OF SHEAR COMPRESSION THEORY

The method proposed in Progress Reports 17 and 17A<sup>(1,2)</sup> proved to be inadequate when comparisons were made with experimental results, as can be seen from Fig. 32. This led to the decision to attempt a revision of the method to increase its accuracy. In order that the reader will not have to refer back to the original reports, the shear compression theory will be summarized in subsequent paragraphs.

### Basic Concept of the Shear Compression Theory

The fundamental concept of the theory lies in the compatibility condition which states that deformations in the zone of inclined cracking result from a "shear rotation" about a neutral axis of the failure section when the concrete in a region above the inclined crack reaches a limiting state of stress determined by the Mohr failure criterion.

### Development of the Shear Compression Theory Equations

A brief discussion of the theory will be undertaken with the aid of Fig. 33 which consists of an elevation

view and an end view of a typical beam, together with a free body diagram of the segment to the left of the critical section.

Failure is impending and a large crack has formed denoted by B'O'C in the elevation view of Fig. 33. The crack formation is accompanied by a rotation about the point O' such that the angle B'O'C, subtended by the exposed reinforcing steel, is assumed equal to the angle A'O'D. The angle A'O'D defines the amount of compressive deformation of the longitudinal fibers of the concrete above and to the left of the point of rotation O'. The value  $\Delta \ell_{\text{top}}$  was approximated by evaluating the total strain in the top fibers from the point A' to a point above point B'. The value  $\Delta \ell_{\text{bot.}}$ , on the other hand, was obtained by utilizing data from pull out tests involving various types of reinforcement embedded in concrete cylinders. Bond coefficients were employed to evaluate the three types of reinforcement considered, namely plain round bars, deformed bars, and prestressing strands.

A consideration of the free body diagram in Fig. 33 will facilitate derivation of the equation for the moment,  $M_{su}$ , at impending shear compression failure. The diagram



shows the critical combination of forces  $V_u$ ,  $C_u$ , and  $T_u$  at failure, and in addition an internal concrete normal stress,  $\sigma_o$ , is depicted. The stress  $\sigma_o$  is assumed to be uniform over an area defined by the distance,  $h_1$ , measured from the top fiber. The distance  $h_1$ , also locates the center of rotation,  $O'$ . The equation expressing the internal bending moment is

$$M_{su} = C_u \left( h - \frac{h_1}{2} \right) \quad (1)$$

Recognizing that the term,  $C_u$ , is equal to the product of the uniform stress,  $\sigma_o$ , and the area acted upon,  $b \cdot h_1$ , Eq. (1) becomes

$$M_{su} = \sigma_o b h_1 \left( h - \frac{h_1}{2} \right) \quad (2)$$

Finally, after regrouping terms,

$$M_{su} = \sigma_o b h^2 \left( \frac{h_1}{h} \right) \left[ 1 - \frac{1}{2} \left( \frac{h_1}{h} \right) \right] \quad (3)$$

The value of  $M_{su}$  can be calculated if expressions for  $\sigma_o$ , and  $h_1/h$  are obtained. The mean limiting compressive stress,  $\sigma_o$ , is based on the Mohr failure criterion. The essence of this criterion is that failure will occur in the concrete when a combination of shearing and normal stresses reach certain values defined by Mohr's

envelope of failure. The derivation results in the following expression for  $\sigma_o$ ,

$$\sigma_o = \frac{f'_c}{1 + 3 \left( \frac{Vh}{M} \right)^2} \quad (4)$$

where  $f'_c$  is the strength of a 6 x 12 in. concrete cylinder, and  $V/M$  is the shear-moment ratio, assumed to be constant for any given loading mode. The value of  $\sigma_o$ , for a given strength of concrete, thus depends on the ratio  $V/M$  corresponding to the applied loading. The value of  $h_1/h$  is found by consideration of equilibrium for the free body of Fig. 33, and the assumption of equal angles  $B'O'C$  and  $A'O'D$  previously discussed. The final result is

$$\frac{h_1}{h} = \frac{1 + 0.75\epsilon_o \sqrt{\frac{\sin\alpha \cdot \tan\alpha}{\epsilon_{cu} \cdot h}}}{\frac{0.75}{pE} \sigma_o \sqrt{\frac{\sin\alpha \cdot \tan\alpha}{\epsilon_{cu} \cdot h}} + 1.65} \quad (5)$$

where

$\epsilon_o$  = effective prestressing strain in the steel plus elastic strain in the concrete at point of resultant force in the prestressing steel

$E$  = modulus of elasticity of the steel

$p$  =  $A_s/bh$

$A_s$  = area of steel

$\alpha$  = angle of inclination of failure crack

$\epsilon_{cu}$  = ultimate concrete strain

$\lambda$  = 10,000  $\lambda'$

$\lambda'$  =  $(0.5 + \frac{2500}{F'_c}) K'd$

$d$  = bar or strand diameter

$K'$  values for reinforcing steel were given in Progress Report 17A as follows:

	<u>Non-rusted</u>	<u>Rusted</u>
Plain round bars	5.5	4.0
Deformed bars	3.0	2.0
Prestressing strands	2.0	1.5

If it is assumed that the values of  $\alpha$  and  $\epsilon_{cu}$  are 45 degrees and 0.0036, respectively, then

$$\frac{h_1}{h} = \frac{1 + 10.5 \epsilon_o \sqrt{\lambda/h}}{10.5 \frac{\sigma_o}{pE} \sqrt{\lambda/h} + 1.65} \quad (6)$$

Thus the value of the ultimate moment,  $M_{su}$ , can be calculated using the above equations and appropriate parametric values.

#### New Evaluation of Bond Parameter

A study of the theory revealed that the bond parameter,  $\lambda$ , is the largest single uncertainty. It was shown in Progress Report 17 that

$$\frac{\lambda'}{K'd} = \left( 0.5 + \frac{2500}{f'_c} \right) \quad (7)$$

where  $\lambda'/K'd$  is presumably a function of the concrete strength. An examination of Fig. 34, wherein the relationship expressed by Eq. (7) is plotted, indicates a considerable scatter of values and corresponding lack of correlation.

Fortunately, ultimate moment values are quite insensitive to small variations in the bond parameter and the  $\lambda$  value for a given type of reinforcement can be chosen as the average value from many beam tests. These values were actually calculated by working back from experimental results. With  $M_{su}$  known from tests, and solving Eq. (3) as a quadratic in  $h_1/h$ , we get

$$\frac{h_1}{h} = 1 - \sqrt{1 - \frac{2M_{su}}{\sigma_o b h^2}} \quad (8)$$

From Eq. (6), it can be shown that

$$\frac{\lambda}{h} = 0.00907 \left[ \frac{1 - 1.65 \frac{h_1}{h}}{\frac{\sigma_o}{pE} \frac{h_1}{h} - \epsilon_o} \right]^2 \quad (9)$$

If the term  $\mu$  is denoted as a new bond parameter, such that

$$\mu = \frac{\lambda}{10,000 d} = \frac{\lambda'}{d} \quad (10)$$

then it will be possible to obtain these  $\mu$  values knowing that

$$\frac{\lambda}{d} = \frac{\lambda}{h} \cdot \frac{h}{d} \tag{11}$$

More specifically, from beam test data it is possible to successively evaluate  $h_1/h$  and  $\lambda/h$  from Eqs. (8) and (9), respectively; after which  $\lambda/d$  and finally  $\mu$  is found by means of Eqs. (11) and (10), respectively. Available data, shown in Fig. 35, resulted in the following average values of  $\mu$  :

- (a) Structural grade deformed bar.....2.73
- (b) Prestressing strand.....0.32
- (c) Prestressing wires, individually bonded.....0.96

#### Compatibility Condition Reviewed

The compatibility condition or idealized mechanism of failure proposed in the theory was investigated in conjunction with several of the beam tests in an effort of establish its validity. This mechanism may be briefly described as a rotation about the end of the principal inclined crack in the region of failure.

Beams of Series C were chosen for this study and

the procedure was to photograph the crack pattern during the final loading increments. Measurements on the photographic print of relative movement of reference points adjacent to the principal crack enabled the establishment of the actual center of rotation for each of the beams. The study revealed that the center of rotation is not at the end of the inclined crack (Point 0' in Fig. 33), but about a point which is approximately at the same elevation as the top of the crack and several inches from point 0' in the direction of increasing moment. The rotation can actually be resolved into two components. One is a rotation about 0', as postulated in the theory, and the second is a vertical displacement. The fact, however, that the observed location of the point of rotation was near the end of the diagonal crack, led to the conclusion that the compatibility condition from which Eq. (5) is derived does not require revision and may be used in its original form. Therefore the revision of the theory centered about the bond parameter  $\lambda$ .

#### Discussion of Limiting Stress

The method being considered is a shear compression theory that predicts the strength of a member when the

concrete above the end of the diagonal crack crushes, or is incapable of carrying additional loading. This limiting stress or crushing stress is called  $\sigma_0$  and is dependent on the magnitude of the normal and shear forces, as indicated by Eq. (4). The effect of the shear force is to reduce the normal force needed to crush the concrete. However, at ultimate load, the beams tested during this investigation did not necessarily behave in accordance with the shear compression theory. For example, there were cases where failure occurred in crushing of the concrete inward of the load point, in a region of zero shear. For example see view of Beam C4 in Fig. 25. In this instance the limiting stress should have equalled the cylinder strength and not some lesser value given by Eq. (4), since the shear force is zero in the region between the load points. However, in this investigation it was assumed that Eq. (4) was valid in all cases regardless of the location of final crushing.

## COMPARISON OF REVISED THEORY WITH TEST RESULTS

Figure 32 shows values of ultimate moment, calculated by the original as well as the revised method, compared with the experimental results of several investigations.<sup>(3,6,7,8,9)</sup> The points referred to as "original theory" were computed by means of Eqs. (7), (6), and (3); while those referred to as "revised theory" were computed by Eqs. (11), (6) and (3) using the modified  $\mu$  values. This figure generally shows an increase in correlation and a decrease in scatter when the original theory is compared to the revised one. Exceptions are the tests of Zwoyer<sup>(6)</sup> and Clark<sup>(9)</sup>. In these cases the scatter was slightly increased with application of the revised theory.

The results of the beam tests reported herein were not all used in the comparison shown in Fig. 32. Results from tests of Beams C3, C4, C12, C15, and C16 were excluded because it was apparent that their short shear span precluded any possible diagonal tension failure and consequently forced failure either in flexure or bond. Beams C6 and C10 were excluded because they were tests to determine the effect of reloading. All of the D-Series of tests, except Beams D1 and D4, were excluded because of the fact that the loading had been transmitted by stubs.



It must be concluded that whereas the revised theory does, indeed, seem to reduce the discrepancy between the calculated results and the corresponding experimental values for the numerous investigations considered, there is still need for further improvement.

## DISCUSSION OF CONDITIONS AFFECTING ULTIMATE STRENGTH

Beams tested in this investigation were used to ascertain the effect of length of overhang at the reaction, the influence of existing inclined cracks, and the height of load point, on ultimate strength. The beams, designated as Series C, and loaded as shown in Table I, were used to evaluate effects of length of overhang and existing inclined cracks. The height of load point was the main variable in the testing of the beams of Series D, as outlined in Table II.

A detailed analysis of these tests and the results obtained follows.

### Length of Overhang

#### General

A short overhang may produce two different effects that tend to lower the ultimate strength of a prestressed concrete beam. First, a short overhang may cause the prestress transfer zone to be positioned on the test span in a region of high shear. Within the prestress transfer zone the concrete is subjected to smaller compressive

stresses than at other sections of the beam and hence lower resistance to cracking and shear. Second, a short overhang may result in a bond failure of the reinforcement due to inadequate embedment.

The first group of 12 beams in Table I contains six beams with overhangs of 2-1/2 in., and six with overhangs of 24 in. The main variables were type of reinforcing, intensity of prestress, and shear span. The reinforcing was either prestressing strands or deformed bars. Strands in Beams C5, C8, C9, and C12 had effective prestress values of 52,600 psi, 54,400 psi, 49,100 psi, and 46,200 psi respectively, while Beams C1, C2, C3 and C4 were essentially without prestress. The remaining four beams, C13, C14, C15, and C16, were made with non-prestressed deformed bars. The shear spans were either 18 in. or 30 in., except for Beam C9 which had a 27 in. shear span.

#### Effect of Type of Reinforcing

The study of the effect of the type of reinforcing is summarized in Table VI, which contains a re-grouping of data from Table V and also gives computed ultimate loads based on the shear compression theory<sup>(1,2)</sup>, and

on a method based on a condition of pure flexure.<sup>(10)</sup>

The data in Table VI are divided into two groups. Group I contains beams with a 30 in. shear span and Group II beams with an 18 in. shear span. Each group includes two beams with 24 in. overhang beyond the supports and two with 2-1/2 in. overhang. One beam of each pair was reinforced with untensioned strands and the second with conventional reinforcing bars. Figures 21, 23, 25 and 26 show photographs of all beams listed in Table VI after testing to ultimate load.

The results in Table VI indicate that the shear compression theory works reasonably well for a 30 in. shear span for both types of reinforcing. It is not possible, however, to compute with any practical degree of accuracy the ultimate load based on the assumption of pure flexure, as evidenced by the ratios of  $V_u:V_{BA}$  which range from 0.64 to 0.94 for the four beams of Group I. The observed failure modes indicated shear compression for Beams C1 and C2 reinforced with unprestressed strands, and diagonal tension for Beams C13 and C14 with deformed bars. The length of overhang was significant for Beam C14. It appears from Fig. 23 that the cause of failure

in C14 was a splitting along the reinforcement at the end of the beam, thereby reducing the ultimate strength and explaining the poor correlation with computed values.

The beams of Group II, in Table VI, with the exception of Beam C4, failed in flexure. Beam C4 might also have failed in flexure had not a breakdown in bond occurred. The computed values of  $V_{BA}$  show good agreement with experimental results, whereas the  $V_W$  values are consistently less than the corresponding test results. The ultimate load of 23.0 kips for C4, loaded on an 18 in. shear span, was well above the corresponding value of  $V_W$ , even though strand slip occurred. In this case it appears that a 2-1/2 in. overhang is not sufficient, and this may be also true for shear spans longer than 18 in.

A general observation, substantiated by Figs. 21 and 23, is that the cracking characteristics of the beams reinforced with conventional deformed bars were consistently more favorable from a practical viewpoint than were the companion beams reinforced with unprestressed strands. This is evidenced by the closer spacing and smaller widths of cracks in the beams reinforced with deformed bars.

Effect of Prestress

The effect of prestress is summarized in Table VII, which is arranged in a form similar to Table VI except that data from only three beams was available in Group II; however a third group is shown consisting of one beam with a 27 in. shear span. The objective here is to compare four beams having an effective prestress of approximately 50,000 psi with three beams having practically no prestress.

The results in Table VII show, as before, that the shear compression theory works reasonably well for beams with 30 in. shear spans and also for Beam C9 with a 27 in. shear span. Computed load values based on flexure theory, on the other hand, are consistently larger than the experimental values for these beams in Groups I and III. The effect of prestressing was to increase the load-carrying capacity of the beams and to change the mode of failure from shear-compression in the unprestressed beams to diagonal tension in the prestressed beams. The ratio of loads at failure of prestressed Beam C5 to unprestressed Beam C1 was 1.22, and the ratio for prestressed Beam C8

to unprestressed Beam C2 was 1.04. The various failure modes may be studied in Figs. 21 through 26.

Table VII further shows that the shear compression theory is not satisfactory for shear spans of 18 in., as is evidenced by the low computed values for Group II. These failures, when slip does not occur, are of the flexure mode and this is substantiated by the good agreement with the calculated value for Beam C3. It is reasonable to believe that if slip had not occurred in Beam C12 its load carrying capacity would have been substantially higher due to the effect of prestressing. This would have been consistent with the trend observed with the beams of Group I, and indicates that a 2-1/2 in. overhang is insufficient for beams loaded on a shear span to total depth ratio of 1.5.

#### Effect of Shear Span

To summarize, it would appear that, for the type of beams tested, a shear span of approximately 30 in. will result in shear compression or diagonal tension failures that can be predicted with fair accuracy by shear compression theory. If the shear span is only 18 in., the flexure theory will predict the ultimate strength with greater

accuracy. This applies whether or not prestressing is employed, provided that strand slip does not occur. In cases when slip occurs, the beams failed at a point intermediate between the computed ultimate loads based on shear compression theory and that of pure flexure. It is reasonable to believe, in these cases, that the loading might have developed the full flexural strength,  $V_{BA}$ , had not slip taken place.

### Conclusions

It was observed that a 24 in. overhang provides adequate embedment for the reinforcement, but that a 2-1/2 in. overhang was inadequate when the test beams were loaded on a shear span to total depth ratio of 1.5.

### Effect of Existing Inclined Cracks

#### General

It is conceivable that bridge members, which are subjected to moving loads, might develop inclined cracks due to the load at one position, but subsequently fail with the load at a different position. Moreover, the beam capacity under such conditions might be less than



would be the case if the loading were applied at a stationary position.

### Results of Tests

Beams C6 and C10 were tested by loading in two stages. In the first stage, loading was applied gradually until one or more inclined cracks had formed. After unloading the jacks were shifted so that in the second stage the beam could be loaded to ultimate with a greater shear span. Loading diagrams are included in Table I, and results of the tests are given in Table VIII. Photographs of the re-loaded beams are shown in Fig. 27, along with comparison beams which were tested in a single stage.

Beam C6 is the first specimen listed in Table VIII and was initially loaded with a shear span of 30 in. A distinct inclined crack formed at a load,  $V_{ic}$ , of 14.7 kips. The comparison beam for this stage of loading is Beam C5, which was loaded without moving the load points to an ultimate load of 15.5 kips. The value of  $V_{ic}$  is 94 percent of the ultimate strength of the comparison Beam C5. Load was then re-applied to Beam C6 and taken to ultimate using a shear span of 36 in. Beam C7 having

a shear span of 36 in., and an observed ultimate strength of 13.2 kips, is used for a comparison beam. The ultimate load for Beam C6 was 11.7 kips, or 89 percent of the strength of Beam C7.

The second reloaded beam, Beam C10, was taken slightly above its inclined cracking load of 16.2 kips, which was 74 percent of the ultimate capacity of comparison of Beam C11. Reloading was accomplished with the shear span increased to 30 in., and the ultimate observed strength was 12.8 kips, which was 83 percent of the capacity of comparison Beam C5.

An examination of Fig. 27 reveals that the failure crack, in the case of the reloaded beams, terminated just outside the final load point. On the other hand, each of the Beams C5 and C7, which were loaded to ultimate in one stage, had the failure crack extend underneath the load point. This behavior is consistent with greater strength.

### Conclusions

The results show that less strength is obtainable under reloading conditions than if loading is carried out

in the conventional laboratory manner with loading in a fixed position. The data indicated ultimate strengths reduced by 11 and 17 percent, with the greater reduction applying to the smaller shear span. The straightforward application of a shear compression theory for this case would be inadvisable.

### Height of Load Point

#### General

A beam with loads applied through connections from cross beams does not develop the vertical compression in the compression zone which tends to restrain the development of inclined cracks, as in the case of loads applied directly on top of the beam.<sup>(11)</sup> Consequently the ultimate strength may be reduced.

#### Results of Tests

These Series D tests comprised a total of 12 prestressed beams, six with rectangular sections and six with I-sections. Details of the beams are shown in Fig. 7, and the manner of loading is indicated in Table II. The six beams with rectangular sections were divided into two

groups such that Beams D1, D2, and D3 were tested with a 30 in. shear span, and Beams D4, D5, and D6 with a 24 in. shear span. The six I-beams were grouped so that Beams D7, D8, and D9 had a shear span of 30 in., and Beams D10, D11, and D12 an 18 in. shear span.

The principal results of the tests, compiled in Table IX, consisted mainly of observed values of ultimate load and are arranged in groups according to shear span. The modes of failure shown in the table may be verified by examination of the photographs in Figs. 28, 29, 30, and 31. A comparison of ultimate loads was obtained for the three loading positions with the load applied directly on top, on full stubs, and on half stubs. To facilitate the comparison, the following ratios were computed:

$$\frac{\text{Top}}{\text{Full Stub}} = \frac{\text{Ultimate Strength with Top Loading}}{\text{Ultimate Strength with Load on Full Stubs}},$$

and

$$\frac{\text{Top}}{\text{Half Stub}} = \frac{\text{Ultimate Strength with Top Loading}}{\text{Ultimate Strength with Load on Half Stubs}}.$$

Table IX shows that in every group of beams except one the ultimate strength was less when load was applied to the half stubs compared with load on the full stubs. Likewise in all instances but one, the ultimate strength

was as great or greater with top loading than with full-stub loading. The exception was Group I, where Beam D1 carried an ultimate load of only 15.0 kips at each load point as compared with Beams D2 and D3 which carried loads of 19.3 and 17.4 kips, respectively. The results of tests on Group I are rather questionable, not only because the ultimate strength of Beam D1 appears to be low, but because some difficulty was experienced during the testing of Beam D3 and the ultimate load obtained is somewhat uncertain. The ratios for Group I, however, are consistent with the ratios found for the other groups, since the ratio for top to full stub loading is smaller than the ratio for top to half stub loading in all of the beam groups shown in Table IX.

The load-deflection relationships are shown for each beam group in Figs. 17, 18, 19 and 20. It is significant that the curves are approximately identical for the three beams within each group.

### Conclusions

The manner and position of load application tends to influence the ultimate strength of beams without web reinforcement. All of the failures, when loading was

applied to stubs, were of the diagonal tension type.

This fact would seem to render shear compression analysis ineffective for such cases.

## SUMMARY

The observed crack patterns for the 16 beam tests of Series C and the 12 beam tests of Series D reported herein were classified into two categories: flexural cracks and inclined cracks. Inclined cracks were further subdivided into flexure-shear and diagonal tension cracks. Flexural cracks are caused by the tensile stresses induced by bending moment. Inclined cracks are caused by the combined effect of shear and bending.

In the rectangular test beams, both types of inclined cracking was observed, i.e. diagonal tension and flexure-shear. A diagonal tension crack may occur in a region previously uncracked, or above a flexural crack, and is characterized by relatively rapid development without substantial increase in load. A flexure-shear crack occurs as an extension of a flexural crack which, in regions of high shear, bends and progresses in the direction of increasing moment. It is considered an inclined crack when a new branch is formed in the region of the bend which progresses rapidly downward in the direction of decreasing moment.

All of the I-beam tests reported herein exhibited diagonal tension type cracking irrespective of the type of loading employed.

Beam failures may be categorized as shear and flexural failures. Shear failures may be of two types, diagonal tension and shear compression. Both types involve the formation of an inclined crack. Only three of the beams tested in this investigation, Beams C1, C2, and D1, were considered to have undergone a shear compression failure. With the exception of six beams that failed in flexure or bond, the remainder were typed as diagonal tension failures.

The shear compression theory proposed in Progress Reports 17 and 17A<sup>(1,2)</sup> was reviewed with particular attention given to the bond parameter, compatibility condition, and limiting stress. The study indicated that the most uncertain aspect of the theory centered about the bond parameter, and the coefficients for structural grade deformed bars, prestressing strand, and individually bonded prestressing wires were revised. This revision was accomplished by utilization of test results from several investigations of pretensioned and conventionally



reinforced members, and made possible a somewhat better correlation between the theoretical and experimental results for the tests considered. In some instances, the revision also brought about a reduction in scatter, as is apparent in Fig. 32.

The analysis based on the revised shear compression<sup>(1,2)</sup> theory was applied to all beams of Series C regardless of the type of failure observed. The results were generally acceptable for beams having a shear span to total depth ratio of 2 or greater. From the tests on an 18 in. shear span it may be concluded that the application of the shear compression theory is unsatisfactory for short shear spans of less than 2 times the overall depth of beam.

The results in tests in Series C to ascertain the effect of length of overhang indicated that a 24 in. overhang provides adequate embedment regardless of type of reinforcement, degree of prestress, or shear span. A 2-1/2 in. overhang proved to be adequate except for beams which were tested using a shear span to total depth ratio of 1.5. In two such tests strand slip occurred resulting in a bond failure. It should be

noted however, that slip did not occur until an extremely high shear force had been imposed on the beam.

In the tests in Series C to determine the effect of existing inclined cracks, the test beams were loaded until inclined cracks formed, after which the load was removed and the load points were repositioned for subsequent reloading to failure. The results indicated that significant reductions in ultimate strength can be effected by a reloading procedure of this type, compared to loading to ultimate in a fixed position. The principal reason for the reduction in strength is apparently due to the fact that the failure crack did not pass under the load point, but instead passed outside so that the restraint due to the vertical compression was lost.

The results of tests on the D Series of beams were to ascertain the affects of height of load point. These tests indicated that the manner of load application does influence the ultimate strength.

In general, beams loaded through stubs such that the load was introduced at the mid-depth of the beam had a lower ultimate strength than beams loaded through stubs

such that the load could be introduced at the top of the beam. Maximum ultimate strength was obtained with loads applied directly on top of the beam.

## ACKNOWLEDGEMENTS

This work has been carried out in the Fritz Engineering Laboratory, under the auspices of the Institute of Research of Lehigh University, as part of an investigation sponsored by the Lehigh Prestressed Concrete Committee (LPCC). The membership of the LPCC at the time the laboratory work was carried out was composed of representatives from the following organizations: Pennsylvania Department of Highways, U. S. Bureau of Public Roads; Reinforced Concrete Research Council; Concrete Products of America, Division of the American Marietta Company; American Steel and Wire Division of U. S. Steel Corporation; John A. Roebling's Sons Corporation; and Lehigh University.

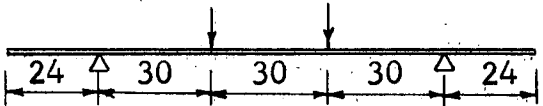


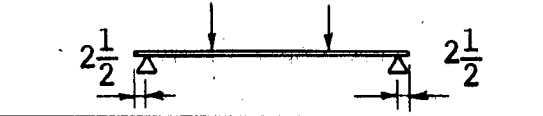
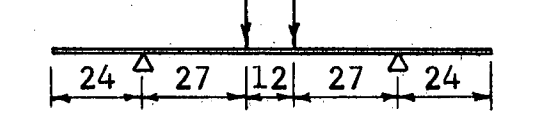
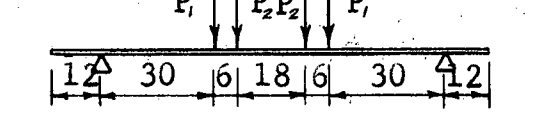
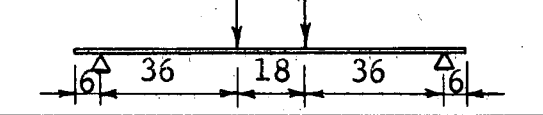
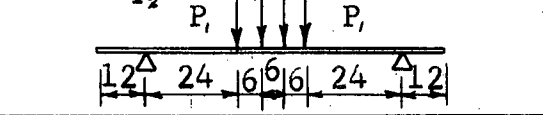
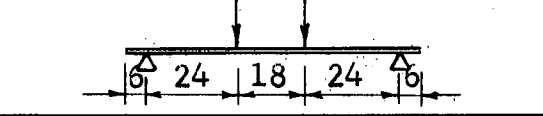
The authors wish to thank Professor William J. Eney, former Director of Fritz Engineering Laboratory, for his encouragement not only with this project but for his sustained interest and help with the prestressed concrete program generally. The present Director of the Fritz Engineering Laboratory is Dr. L. S. Beedle. Valuable assistance in both the manufacture and testing of the specimens was given by Kenneth R. Harpel, Laboratory Foreman, and the

Fritz Laboratory technicians. The prestressing strand was contributed by the John A. Roebling's Sons Corporation and the cement by the Lone Star Cement Company.

TABLES AND FIGURES

Table I

Outline Of Tests For Beams Of Series C

Position Of Loads & Reactions  (All Dimensions in Inches)	Reinforcement			Specific Purpose
	Strands		Deformed Bars	
	Without Pre-stress	Partial Pre-stress		
	C1	C5	C13	Effect  Of  Overhang    Effect Of Existing Inclined Cracks
	C2	C8	C14	
	C3		C15	
	C4	C12	C16	
		C9		
		C6		
		C7		
		C10		
		C11		

Note: P<sub>1</sub> is initial loading position up to the first inclined crack, followed by P<sub>2</sub>, loading in the second position to ultimate.

Table II

Outline Of Tests For Beams Of Series D  
(To Determine Effect Of Height Of Load Point)

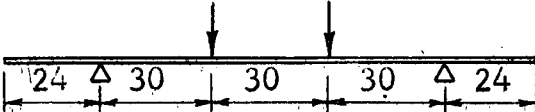



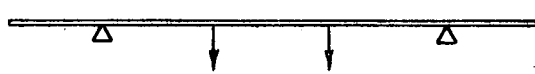
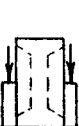
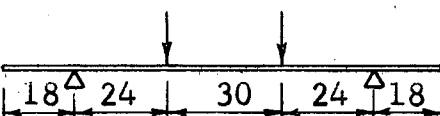


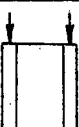
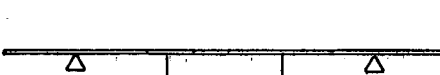
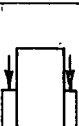
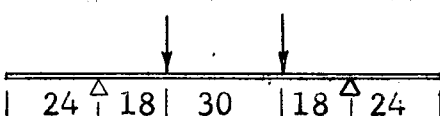

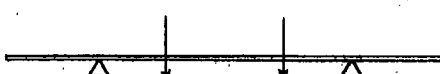



Position Of Loads & Reactions (All Dimensions In Inches)	Load Application	Rect. Section	I Section
		D1	D7
		D2	D8
		D3	D9
		D4	
		D5	
		D6	
			D10
			D11
			D12



Table III  
Prestressing Data and Concrete Strengths  
 (All stresses are in psi)

Beam	Concrete Strength at Test	Steel Stresses		
		Before Release	After Release	At Test
C1	5250	14,000	13,300	6,400
C2	5240	14,000	13,000	5,300
C3	5060	14,000	13,500	5,300
C4	5540	14,000	13,000	5,900
C5	5960	64,800	60,900	52,600
C6	5780	64,800	60,900	55,000
C7	5570	64,800	60,900	50,000
C8	5340	64,800	60,600	54,400
C9	5300	63,100	59,300	49,100
C10	5430	63,100	59,000	49,300
C11	5530	63,100	59,000	48,400
C12	5380	63,100	58,500	46,200
C13	5770	0	0	-3,300
C14	6460	0	0	-2,700
C15	6310	0	0	-3,000
C16	6250	0	0	-3,300
D1	5280	65,000	60,400	45,600
D2	5220	65,000	60,400	51,100
D3	5630	65,000	60,100	45,800
D4	5720	63,200	58,300	42,600
D5	6030	63,200	58,200	44,600
D6	5910	63,200	58,600	43,900
D7	5660	64,900	58,300	39,500
D8	5890	64,900	56,800	39,800
D9	6090	64,900	58,100	41,300
D10	5730	64,700	57,200	40,300
D11	5820	64,700	57,400	40,700
D12	5260	64,700	57,200	39,700

Note: Reinforcement for all beams consisted of four 7/16-in. nominal dia. 7-wire uncoated strands for pretensioning except for Beams C13, C14, C15, and C16, which were reinforced with four No.6 standard deformed bars. Yield strength of deformed bars was 32,900 psi.

Table IV

Beam Dimensions and Test Spans

(All values are in inches)

Beam No.	Breadth b	Effective Depth h	Total Depth D	Overhang $l_0$	Shear Span a	Span $l$	Beam Length L
C-1	6.18	8.62	12.12	24	30	90	138
C-2	6.12	8.68	12.18	2.5	30	90	95
C-3	6.12	8.62	12.12	24	18	66	114
C-4	6.12	8.62	12.12	2.5	18	66	71
C-5	6.12	8.56	12.06	24	30	90	138
C-6	6.12	8.75	12.25	12	30, 36	90	114
C-7	6.12	8.75	12.25	6	36	90	102
C-8	6.18	8.62	12.12	2.5	30	90	95
C-9	6.12	8.62	12.12	24	27	66	114
C-10	6.12	8.62	12.12	12	24, 30	66	90
C-11	6.12	8.50	12.00	6	24	66	78
C-12	6.12	8.68	12.18	2.5	18	66	71
C-13	6.18	8.62	12.12	24	30	90	138
C-14	6.00	8.62	12.12	2.5	30	90	95
C-15	6.06	8.68	12.18	24	18	66	114
C-16	6.12	8.62	12.12	2.5	18	66	71
D-1	6.18	8.56	12.06	24	30	90	138
D-2	6.18	8.75	12.25	24	30	90	138
D-3	6.37	8.68	12.18	24	30	90	138
D-4	6.12	8.56	12.06	18	24	78	114
D-5	6.12	8.56	12.06	18	24	78	114
D-6	6.18	8.62	12.12	18	24	78	114
D-7	6.18	8.62	12.12	24	30	90	138
D-8	6.18	8.62	12.12	24	30	90	138
D-9	6.18	8.62	12.12	24	30	90	138
D-10	6.18	8.62	12.12	24	18	66	114
D-11	6.18	8.62	12.12	24	18	66	114
D-12	6.18	8.62	12.12	24	18	66	114

Note: Beams D7 through D12 are I-Beams. Beams D5, D8, and D11 were constructed with full stubs at load points, Beams D6, D9, and D12 with half-stubs at load points.

Table V

Results of Beam Tests

Beam	Applied Load per Jack in kips At First Crack		Ultimate $V_u$	Ultimate Moment $M_u$ kips-in.	Mode of Failure
	Flexure, $V_{fc}$	Inclined, $V_{ic}$			
C1	3.0	10.0	12.7	381	S (SC)
C2	3.0	10.8	14.5	435	S (SC)
C3	6.0	26.0	30.0	540	F
C4	6.0	14.0	23.0	414	B
C5	6.0	14.6	15.5	465	S (DT)
C6	6.0	14.7	11.7	391	°S (DT)
C7	5.9	12.0	13.2	475	S (DT)
C8	6.0	13.0	15.1	453	S (DT)
C9	7.0	14.0	17.8	481	S (DT)
C10	8.0	16.2	12.8	384	°S (DT)
C11	8.0	16.0	22.0	528	S (DT)
C12	12.0	28.0	29.3	527	B
C13	2.0	12.8	14.2	426	S (DT)
C14	2.0	13.0	13.0	390	S (DT)
C15	5.0	16.0	25.8	464	F
C16	5.0	16.0	26.0	468	F
D1	6.0	12.0	15.0	450	S (SC)
D2	6.0	13.0	19.3	579	F
D3	6.0	12.5	*17.4	522	S (DT)
D4	8.0	22.0	25.0	600	F
D5	8.0	14.0	25.0	600	F
D6	8.0	13.6	21.3	511	S (DT)
D7	8.0	8.5	10.8	324	S (DT)
D8	8.0	7.8	9.6	288	S (DT)
D9	9.0	8.0	9.0	270	S (DT)
D10	10.0	12.5	19.8	356	S (DT)
D11	12.0	8.0	16.5	297	S (DT)
D12	12.0	8.0	15.0	270	S (DT)

\* Faulty Test Procedure

° Beam was Reloaded

Table VI

Effect of Type of Reinforcing

Beam	Overhang in.	Ult. Load $V_u$ , kips	Mode of Failure	Computed Ult. Loads in kips		Load Ratios		Type of Reinforcing (Not prestressed)
				$V_W$	$V_{BA}$	$V_u/V_W$	$V_u/V_{BA}$	
Group I - 30 in. shear span								
C1	24	12.7	S (SC)	13.9	19.8	0.91	0.64	Strands
C13	24	14.2	S (DT)	14.7	15.1	0.97	0.94	Re-bars
C2	2-1/2	14.5	S (SC)	14.0	19.9	1.04	0.73	Strands
C14	2-1/2	13.0	S (DT)	15.3	15.6	0.85	0.83	Re-bars
Group II - 18 in. shear span								
C3	24	30.0	F	15.9	32.1	1.89	0.93	Strands
C15	24	25.8	F	21.9	26.2	1.18	0.99	Re-bars
C4	2-1/2	23.0	B	17.5	33.5	1.31	0.69	Strands
C16	2-1/2	26.0	F	21.7	26.8	1.20	0.97	Re-bars

Note: The symbol  $V_u$  denotes the ultimate load on each jack.  $V_W$  and  $V_{BA}$  denote the corresponding computed loads based on shear compression theory<sup>(1,2)</sup> and on flexure theory<sup>(10)</sup> respectively. Symbols S (SC), S (DT), and F denote shear compression, diagonal tension, and flexural failures, respectively. B denotes a bond failure.

Table VII

Effect of Prestress

Beam	Overhang in.	Ult. Load $V_u$ , kips	Mode of Failure	Computed Ult. Load in kips		Load Ratio		Strand Tension
				$V_W$	$V_{BA}$	$V_u/V_W$	$V_u/V_{BA}$	
Group I - 30 in. shear span								
C1	24	12.7	S(SC)	13.9	19.8	0.91	0.64	No Prestress
C5	24	15.5	S(DT)	17.5	22.7	0.89	0.68	Prestress
C2	2-1/2	14.5	S(SC)	14.0	19.9	1.04	0.73	No Prestress
C8	2-1/2	15.1	S(DT)	16.4	22.1	0.92	0.68	Prestress
Group II - 18 in. shear span								
C3	24	30.0	F	15.9	32.1	1.89	0.93	No Prestress
C4	2-1/2	23.0	B	17.5	33.5	1.31	0.69	No Prestress
C12	2-1/2	29.3	B	20.1	36.8	1.46	0.80	Prestress
Group III - 27 in. shear span								
C9	24	17.8	S(DT)	17.6	24.4	1.01	0.73	Prestress

Table VIII

Effect of Beam Reloading

Beam	First Shear Span, in.	Initial Shear, $V_{ic}$ Kips	Final Shear Span, in.	Ultimate Load, $V_u$ kips	Shear Span in.	Ultimate Load, $V_u$ kips	Comparison Ratios
Group I - Reloaded Beams							
C6	30	14.7	36	11.7			$\frac{14.7}{15.5} = 0.94$ $\frac{11.7}{13.2} = 0.89$
C10	24	16.2	30	12.8			$\frac{16.2}{22.0} = 0.74$ $\frac{12.8}{15.5} = 0.83$
Group II - Comparison Beams							
C5*					30	15.5	
C7**					36	13.2	
C11***					24	22.0	

\*Results compared with  $V_{ic}$  - value for Beam C6 and  $V_u$  - value for Beam C10.

\*\*Results compared with  $V_u$  - value for Beam C6.

\*\*\*Results compared with  $V_{ic}$  - value for Beam C10.

Table IX

Effect of Height of Load Point

Beam	Type of Loading	V <sub>ic</sub> kips	V <sub>u</sub> kips	Mode of Failure	Ratios of Ultimate Loads	
					Top/Full Stub	Top/Half Stub
<u>Rectangular Sections</u>						
Group I - 30 in. shear span						
D1	Top	12.0	15.0	S(SC)		
D2	Full Stub	13.0	19.3	F	0.78	
D3	Half Stub	12.5	17.4	S(DT)		0.86
Group II - 24 in. shear span						
D4	Top	14.0	25.0	F		
D5	Full Stub	14.0	25.0	F	1.00	
D6	Half Stub	13.6	21.3	S(DT)		1.17
<u>I-Sections</u>						
Group III - 30 in. shear span						
D7	Top	8.5	10.8	S(DT)		
D8	Full Stub	7.8	9.6	S(DT)	1.12	
D9	Half Stub	8.0	9.0	S(DT)		1.20
Group IV - 18 in. shear span						
D10	Top	12.5	19.8	S(DT)		
D11	Full Stub	8.0	16.5	S(DT)	1.20	
D12	Half Stub	8.0	15.0	S(DT)		1.32

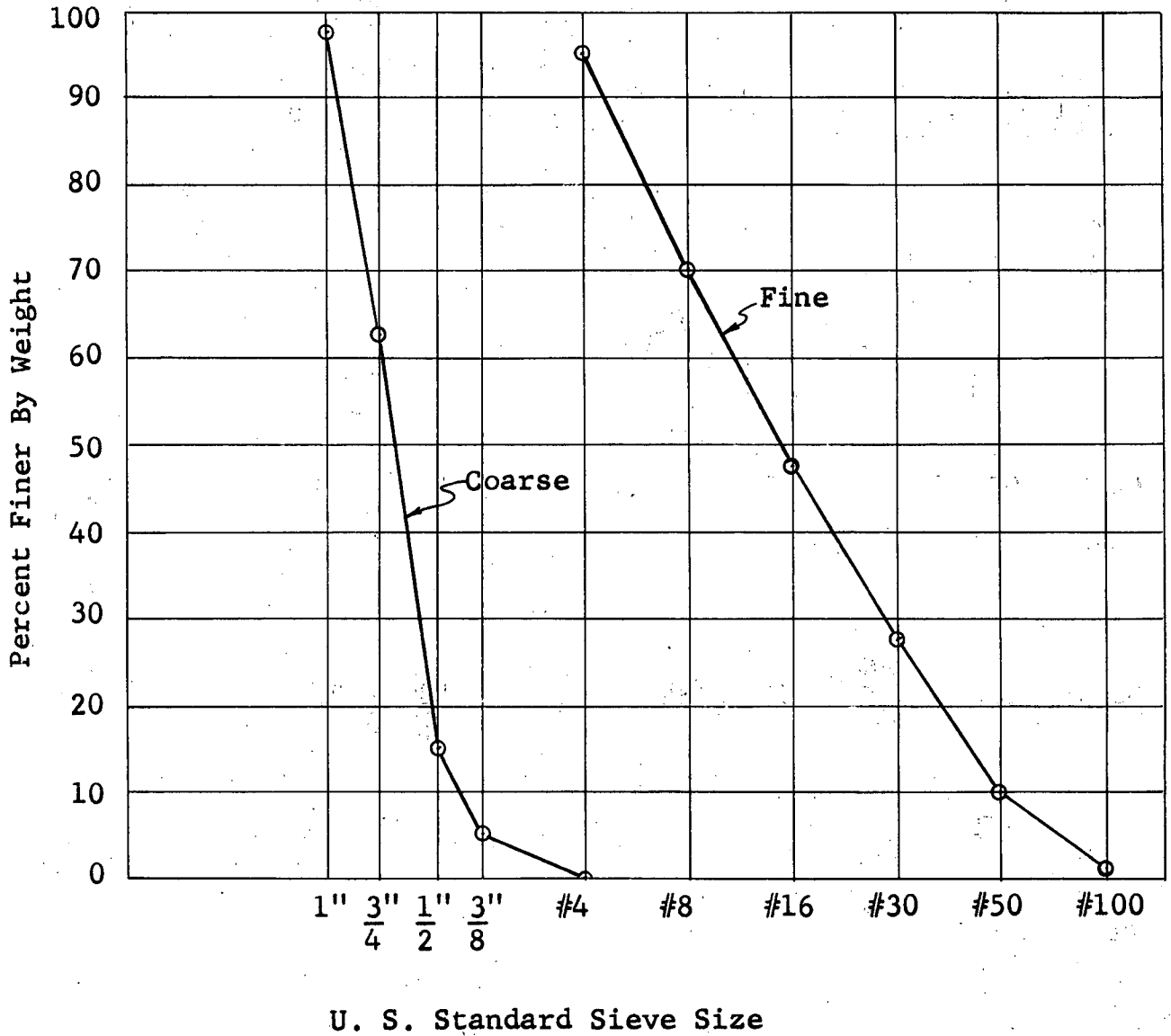


Fig. 1 Gradation of Fine and Coarse Aggregate



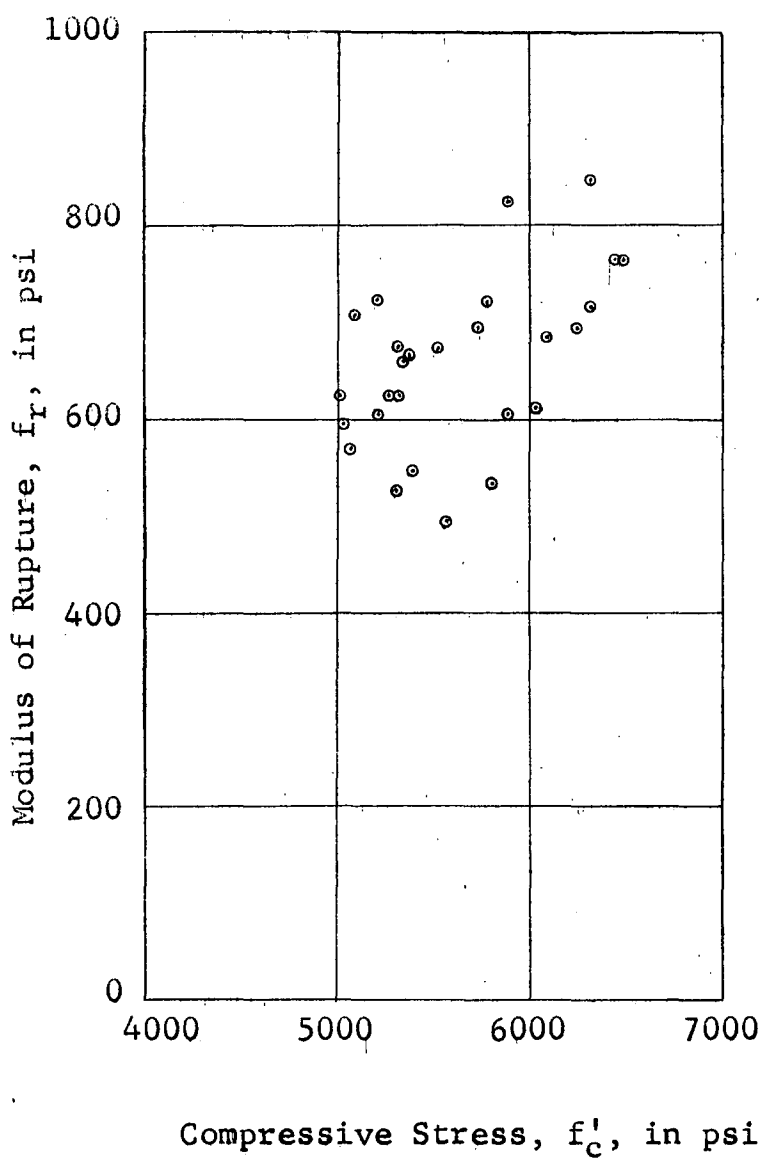


Fig. 2 Relationship Between Rupture Modulus and Compressive Strength

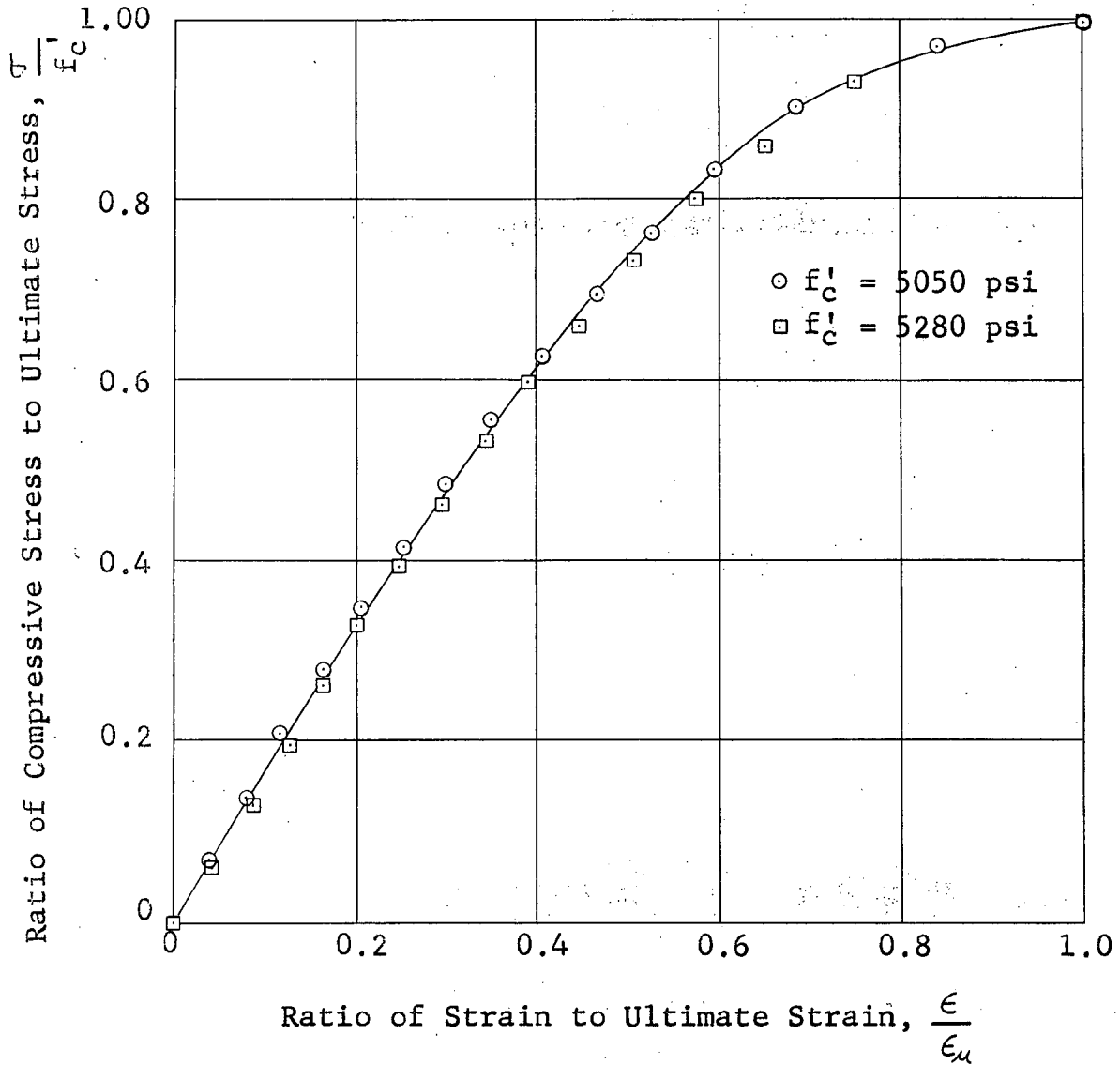


Fig. 3 Stress - Strain Relationship for two 6x12 in. Cylinders

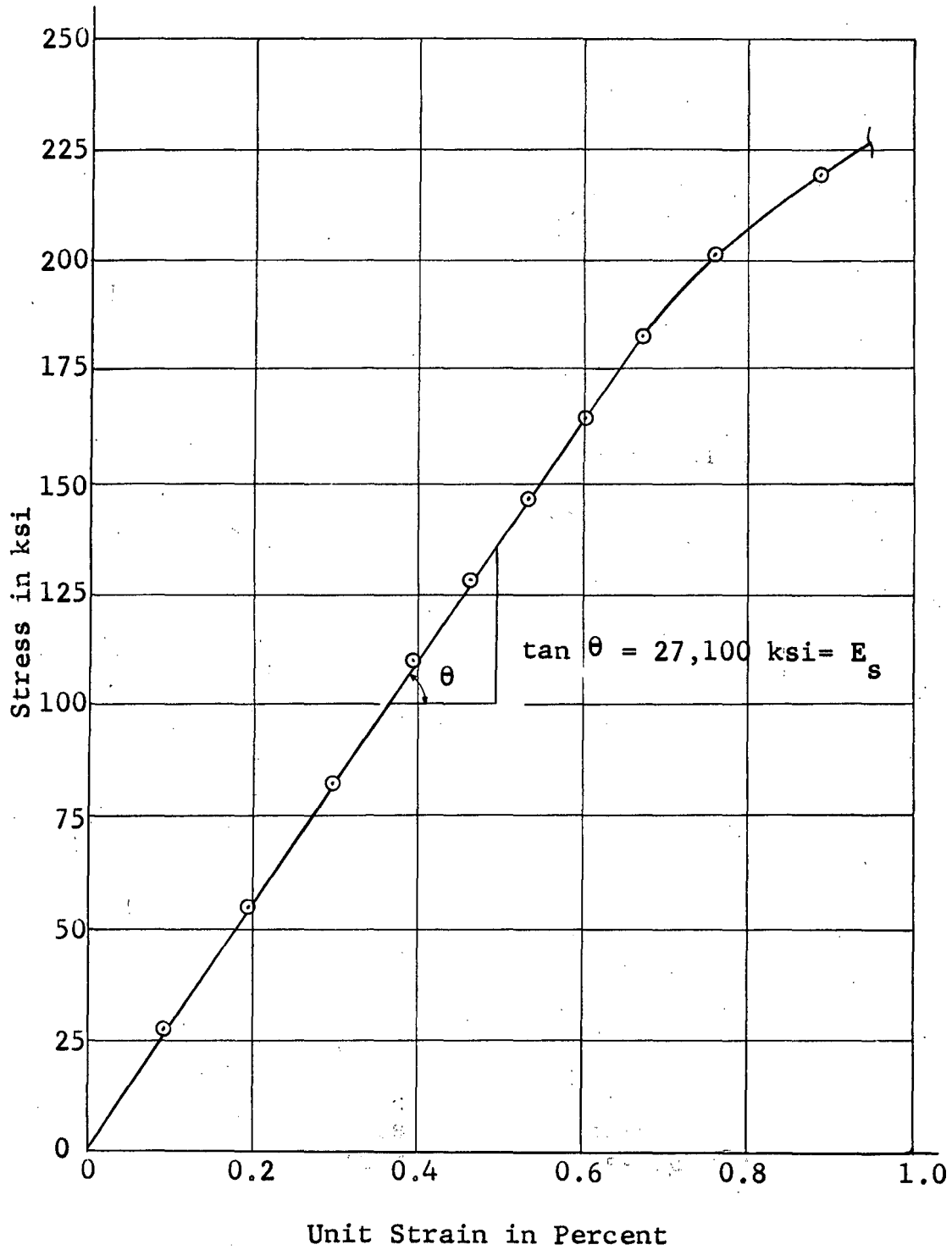
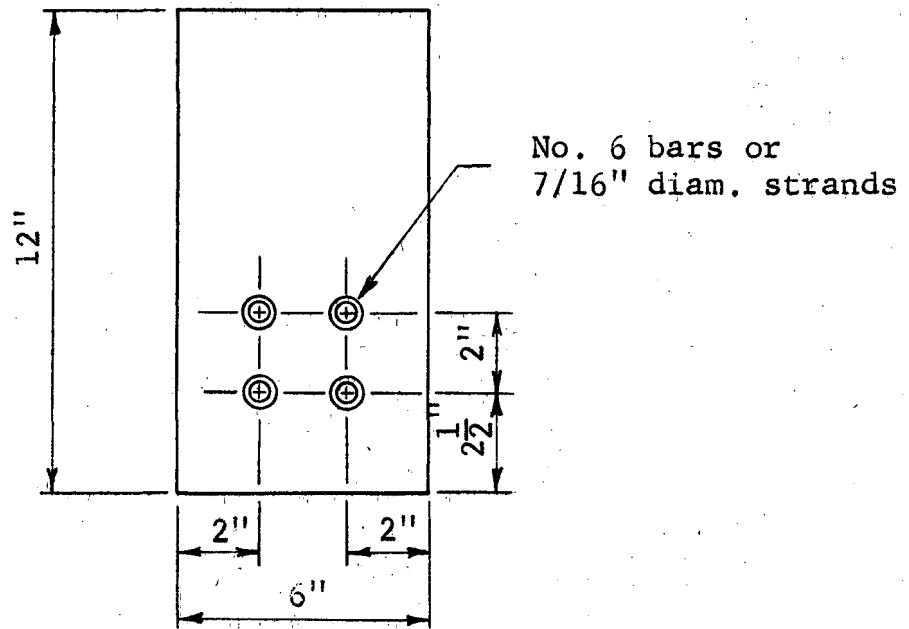
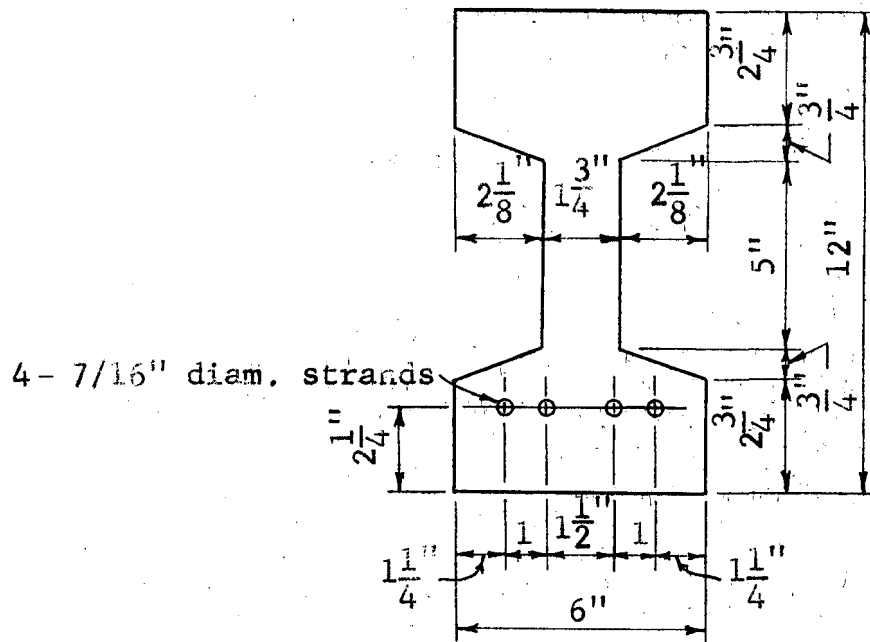


Fig. 4 Stress Strain Relationship for 7/16 diam. Prestressing Strand

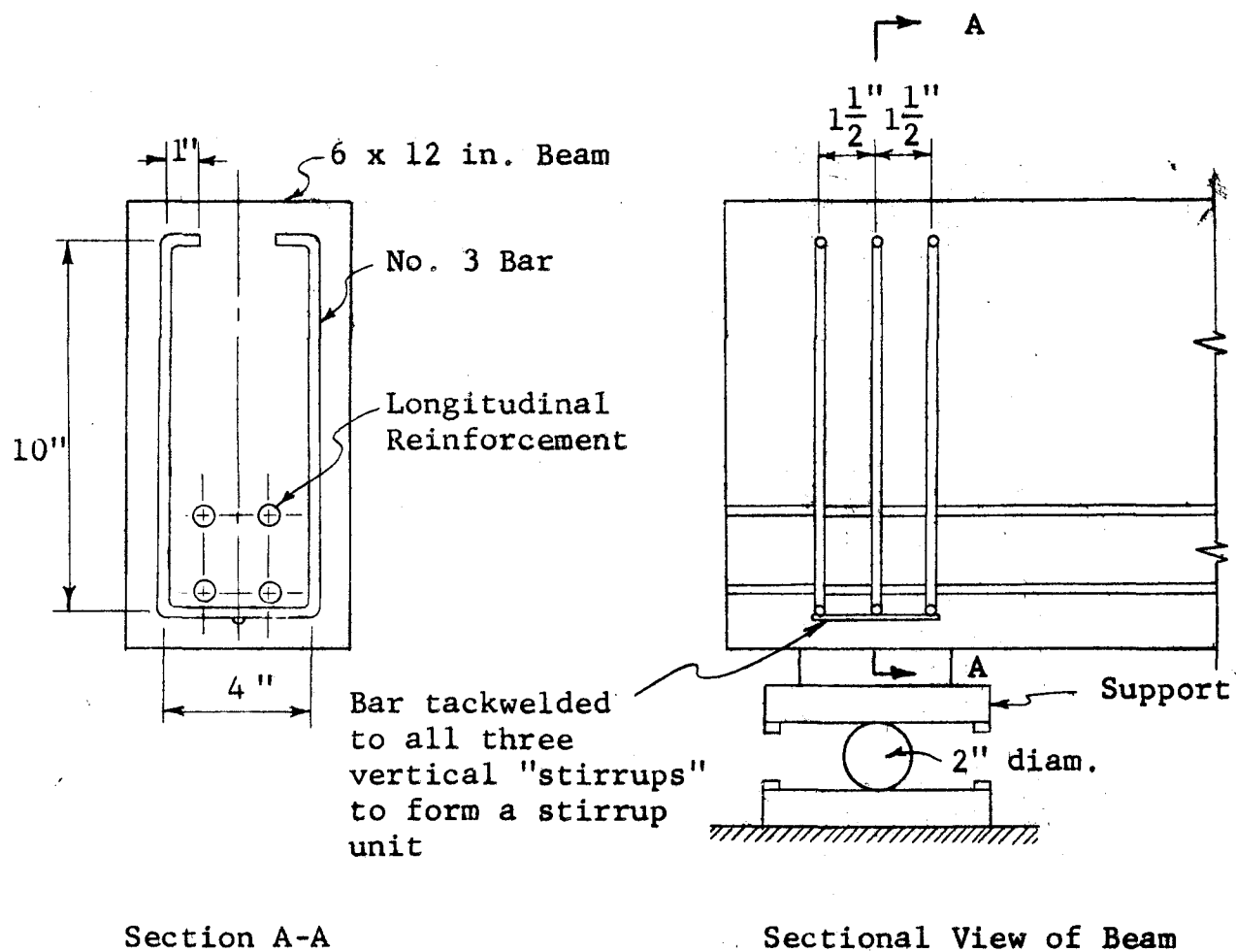


Rectangular Sections



I - Sections

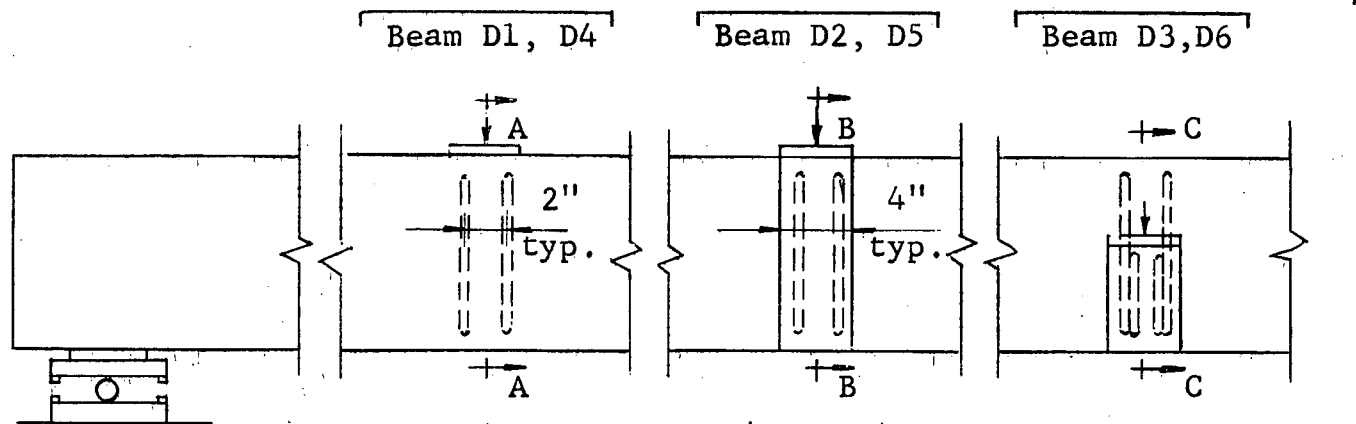
Fig. 5 Nominal Dimensions and Details of Cross-Sections



Note:

A similar group of U-shaped bars was used at each load point in the Series C beams. See Fig. 7 for bar details at load point for Series D beams.

Fig. 6 Typical Web Reinforcing at Supports



Note: All stirrup reinforcement consists of No. 5 bars. Loading jacks are indicated by arrows (†). Under each jack is a steel plate and a layer of neat cement.

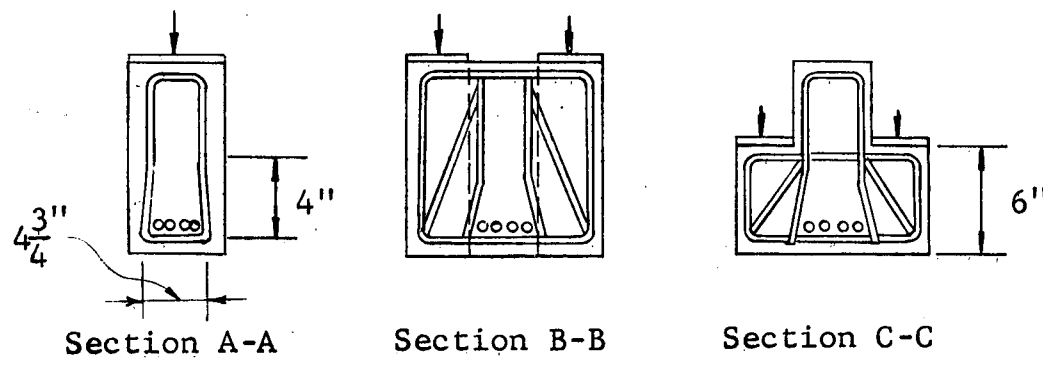
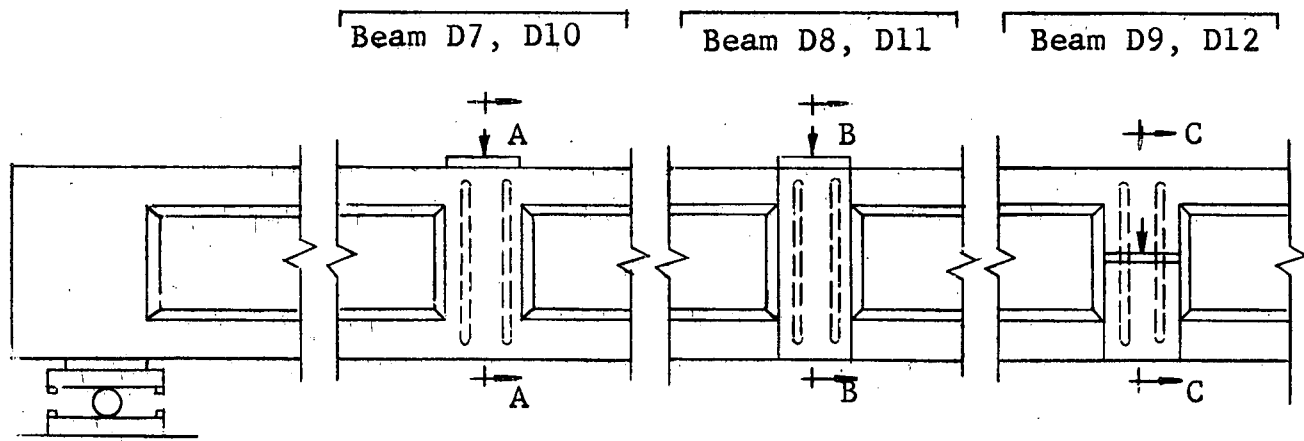
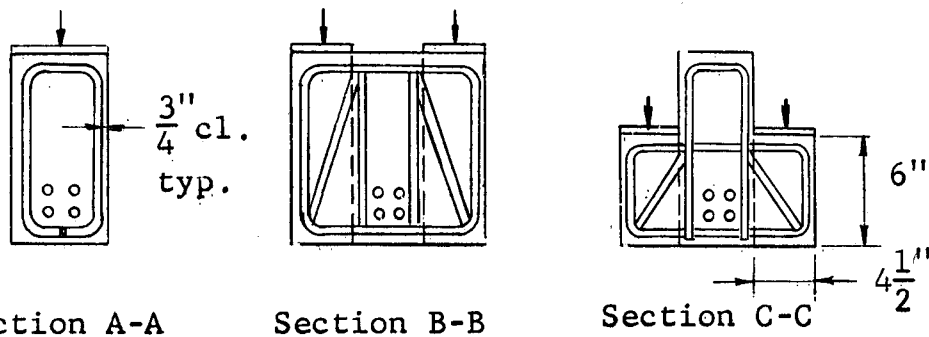


Fig. 7 Web Reinforcement at Load Points for Beams of Series D

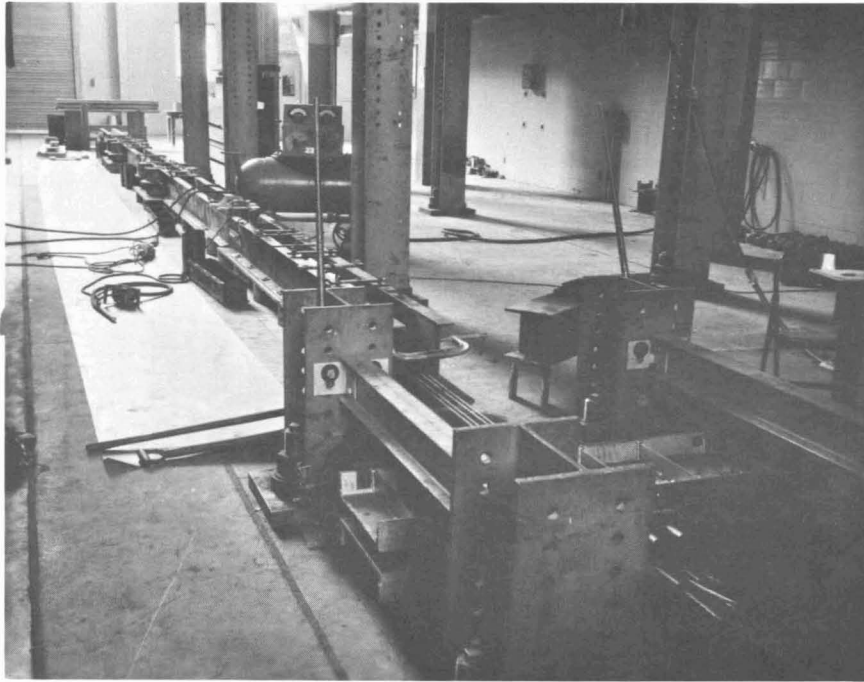
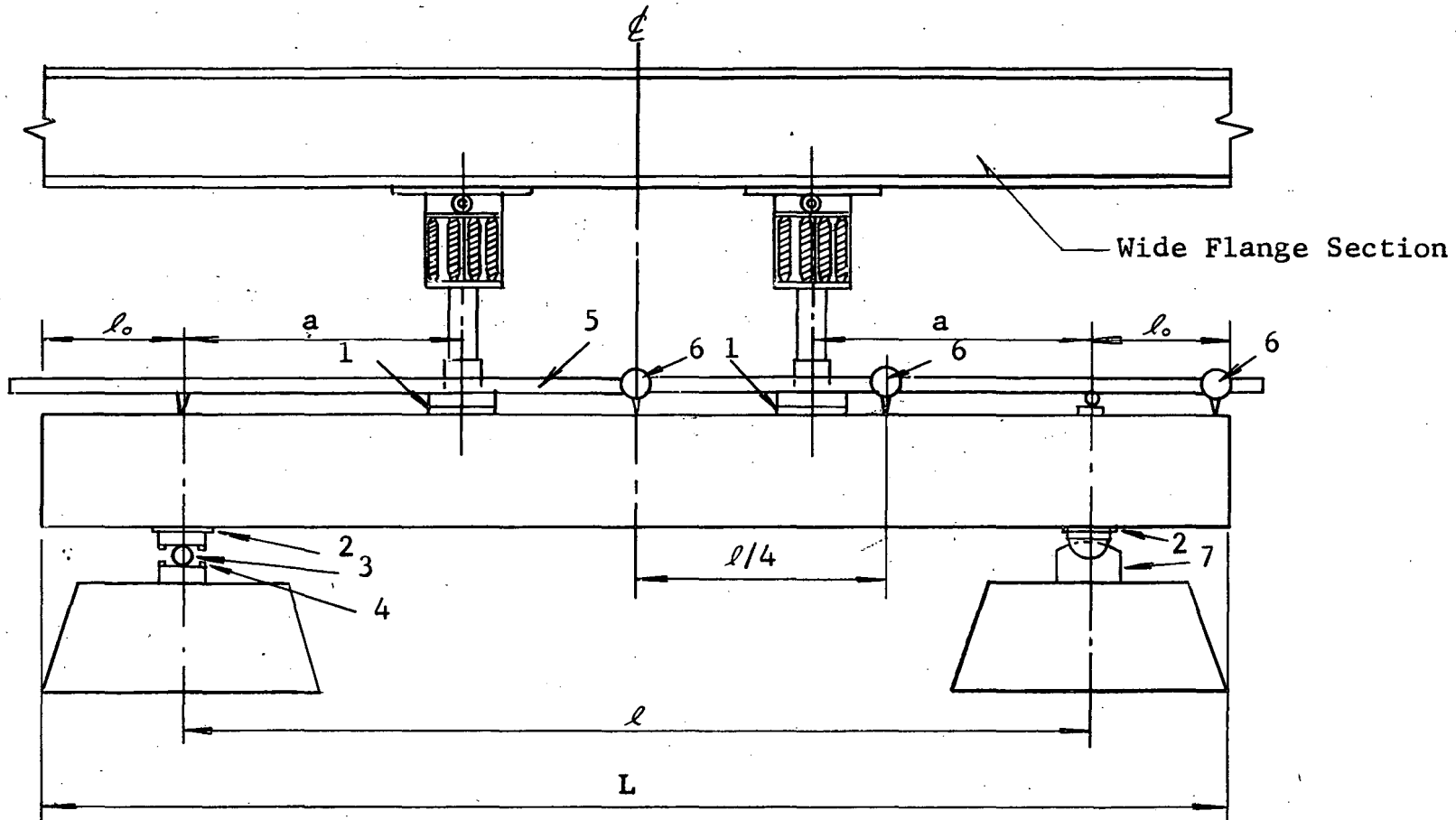


Fig. 8 View Showing Strands Under Tension  
and Forms in Place



1. "Homosote" fibrous hard board, 4x6x1/4 in. thick beneath steel distributor plate, 4x6x1/2 in.

2. Steel distributor plate, 4x6x1/2 in.

3. Steel roller, 2 in. diam.

Note: Dimensions for  $a$ ,  $l$ ,  $l_0$ , and  $L$  are given in Table IV

4. Steel bars, 1/4x1/4x6 in. welded to pedestal to provide horizontal restraint

5. Supporting frame for dial gages

6. Dial gages

7. Hemi-spherical bearing support, 6 in. diam.

Fig. 9 Elevation View of Typical Test Setup



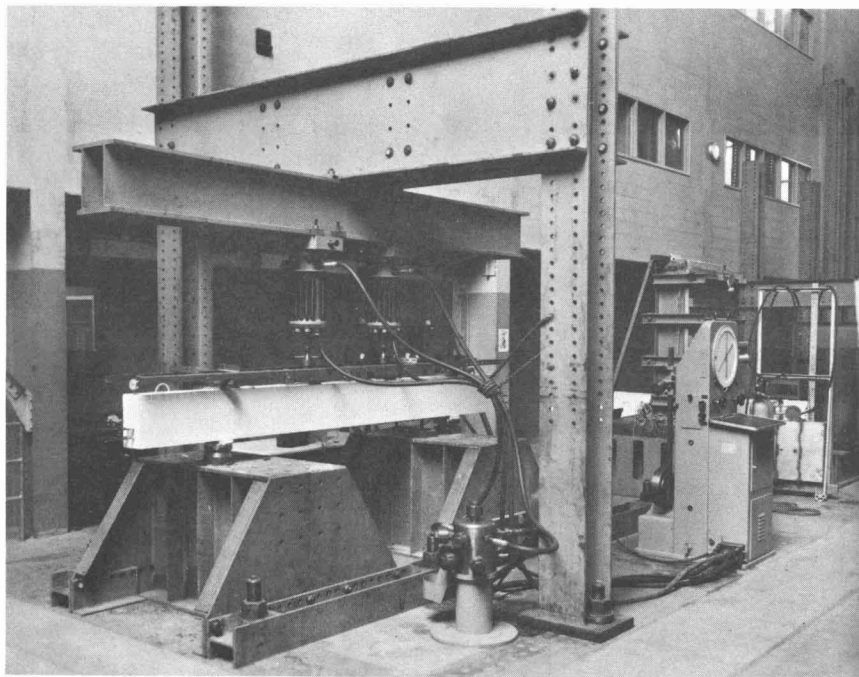
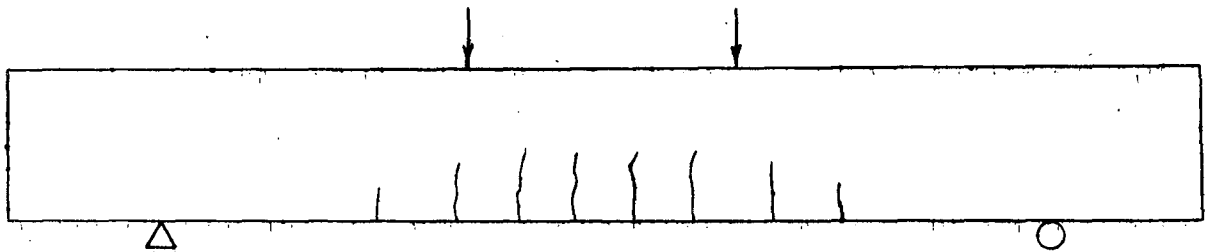
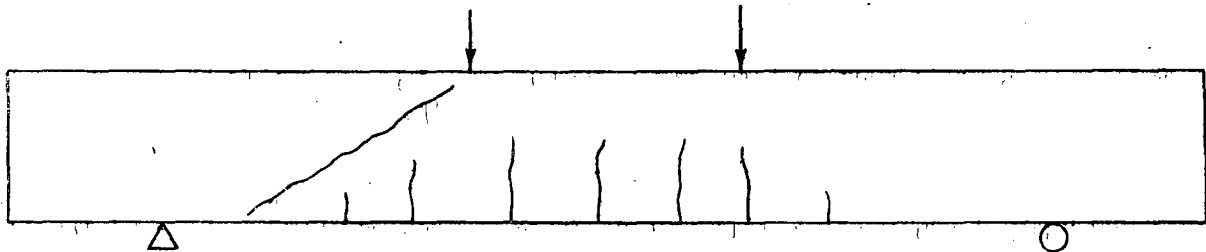


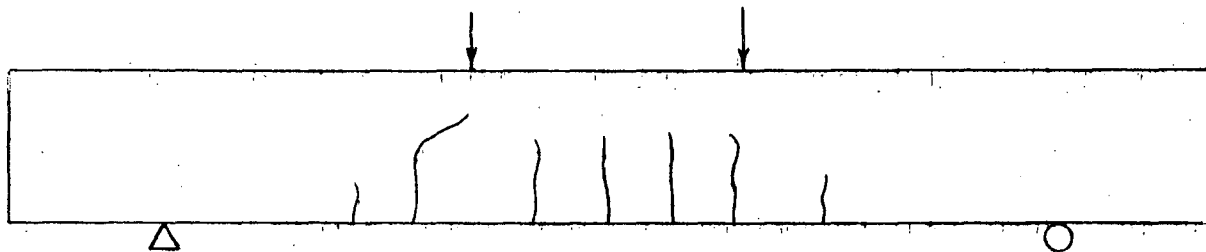
Fig. 10 Photograph of Test Set-up



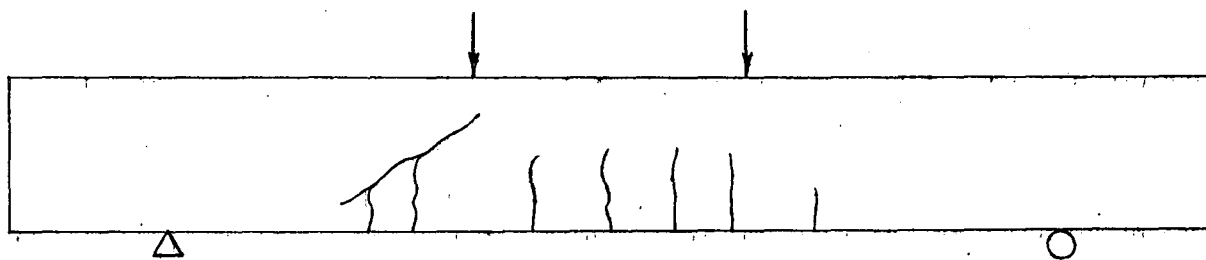
a. Flexure Cracks



b. Flexure Cracks Plus a Diagonal Tension Crack

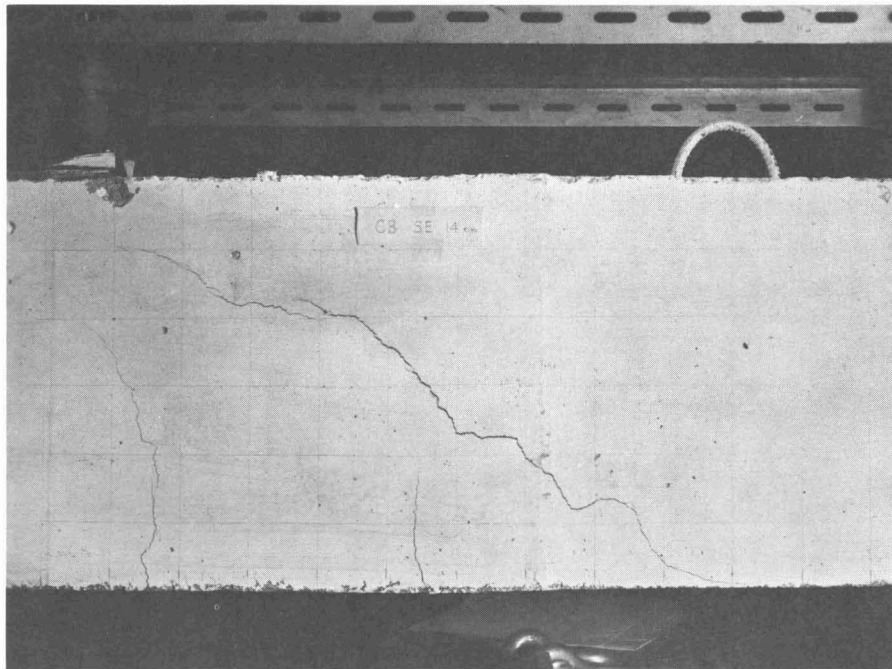


c. Flexure Cracks Plus a Partially Developed Flexure-Shear Crack

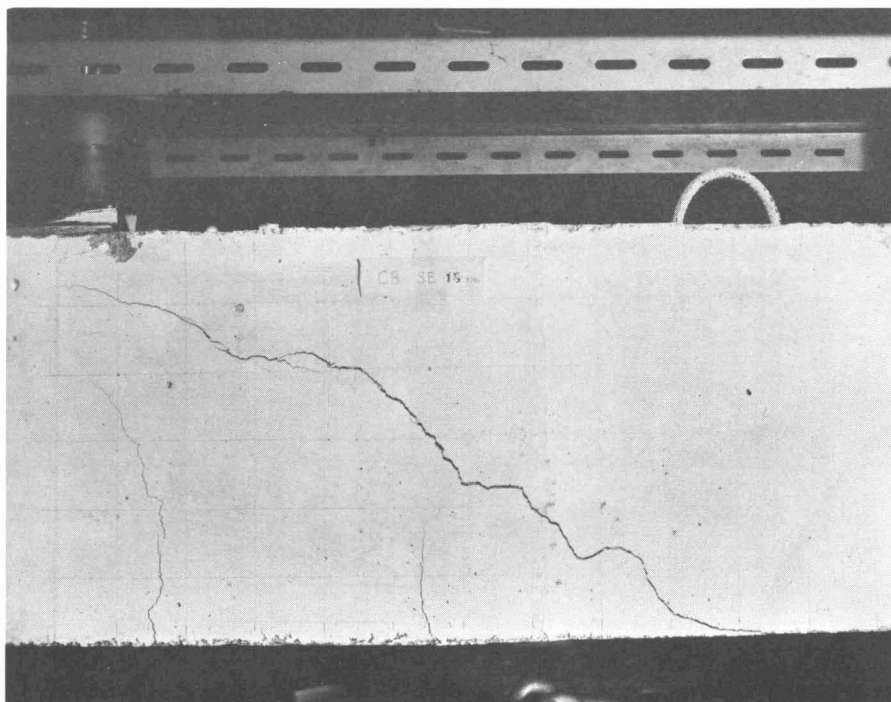


d. Flexure Cracks Plus a Fully Developed Flexure-Shear Crack

Fig. 11 Diagrams Showing Typical Crack Patterns



Load at 14 kips Shear



Load at 15 kips Shear

Fig. 12 Photographs of Beam C8 During Testing

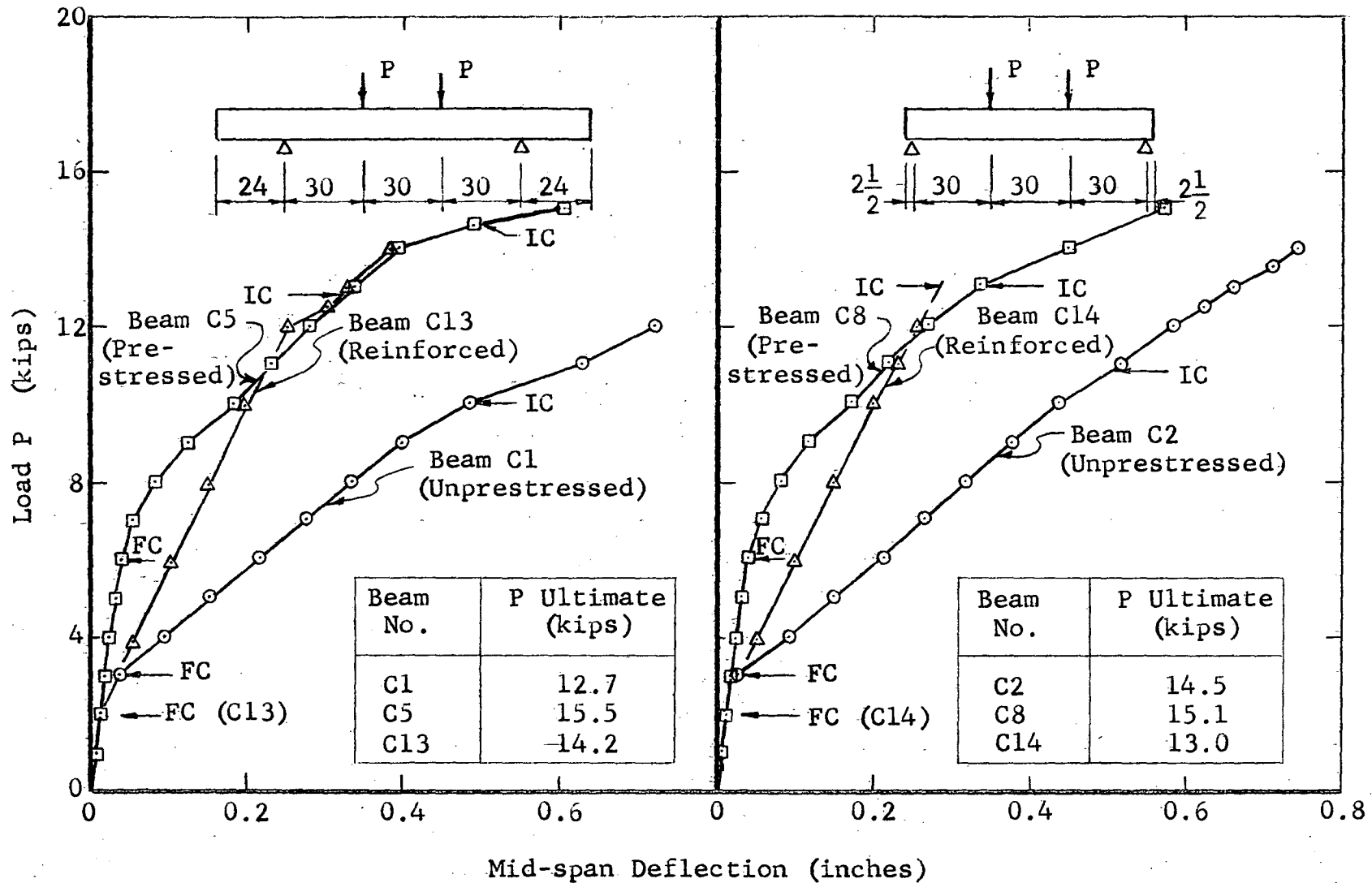


Fig. 13 Load Deflection Curves for Beams C1, C5, and C13, and Beams C2, C8, and C14

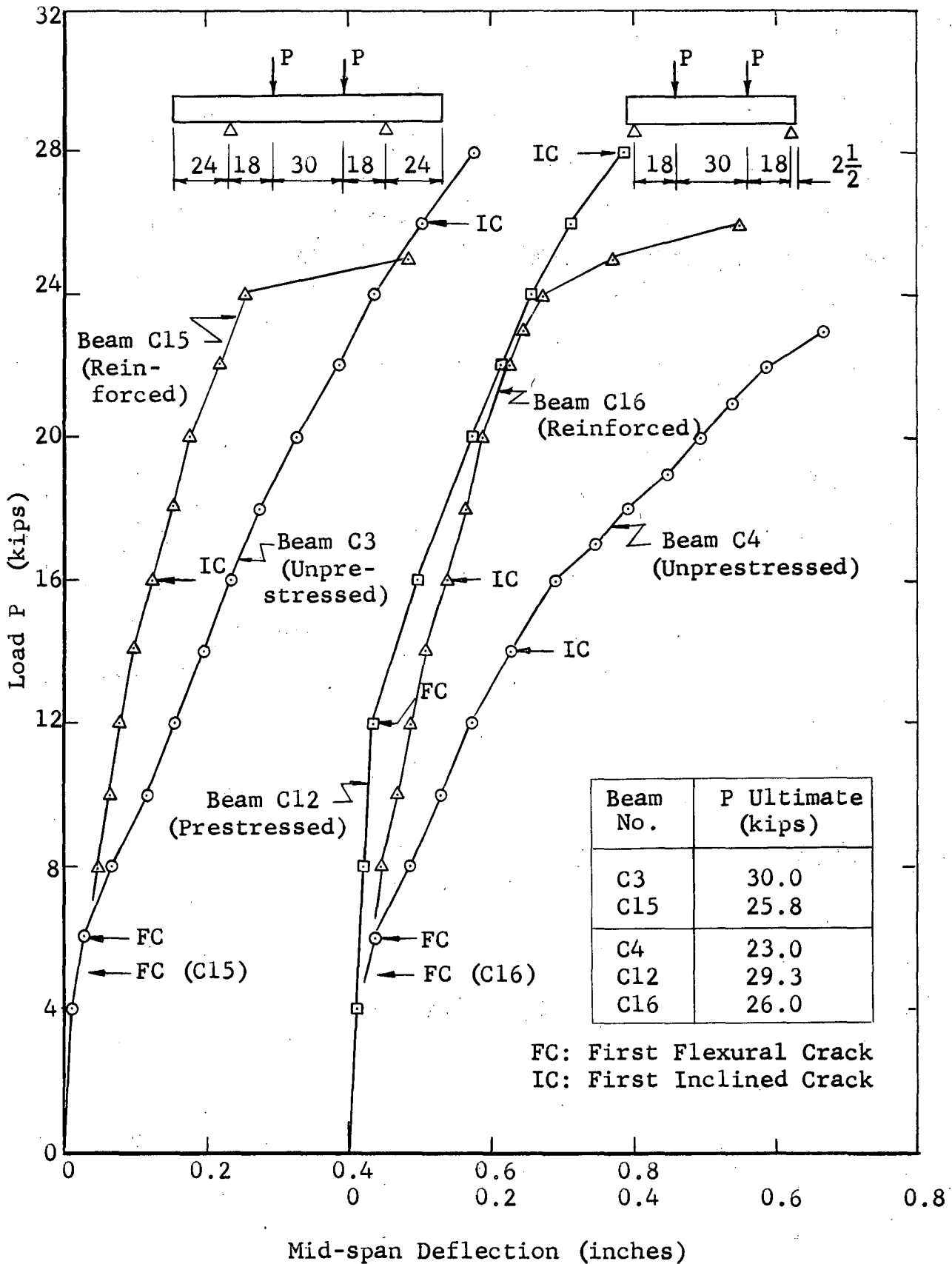


Fig. 14 Load Deflection Curves for Beams C3 and C15, and Beams C4, C12, and C16

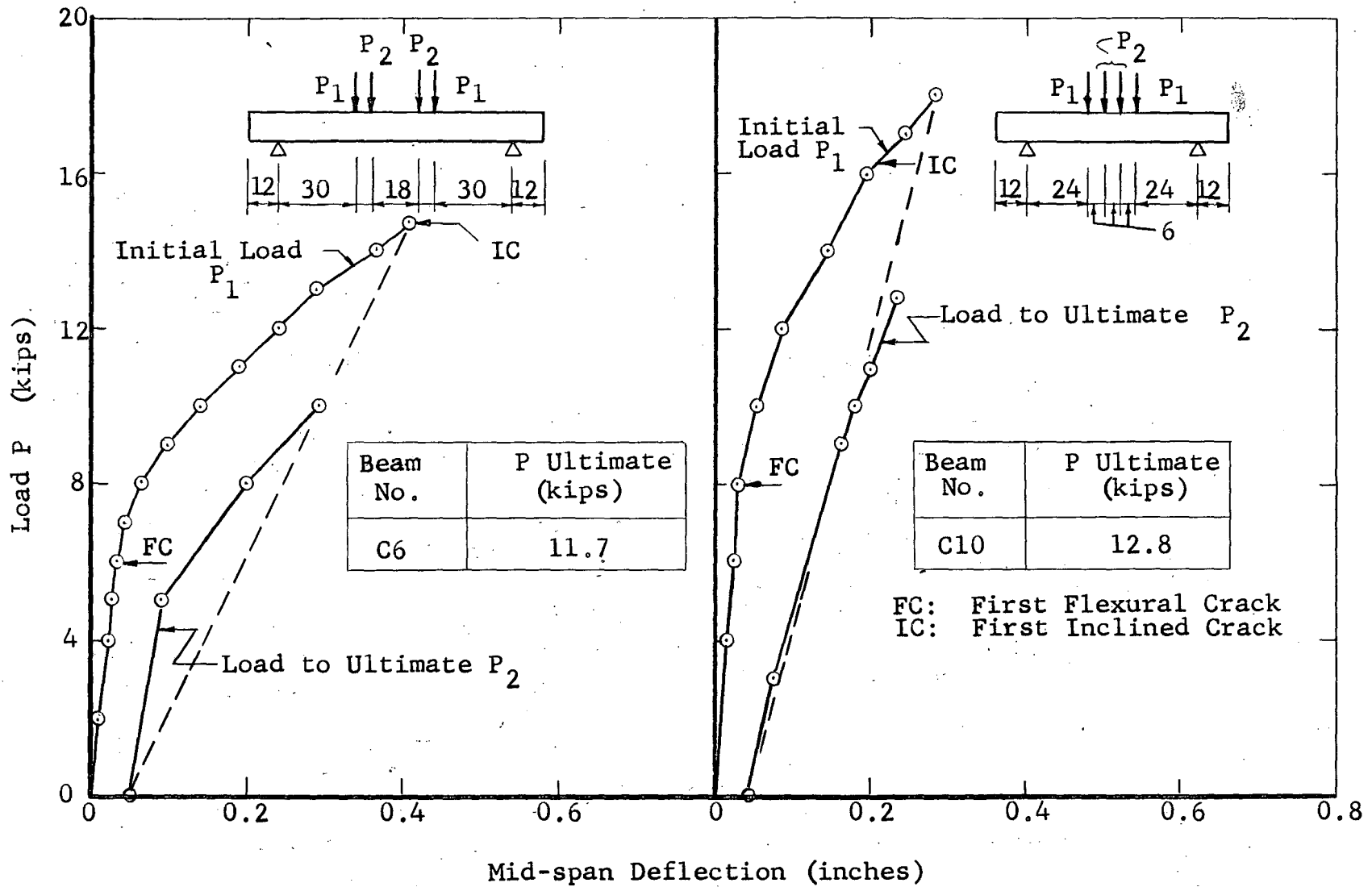


Fig. 15 Load Deflection Curves for Beams C6 and C10

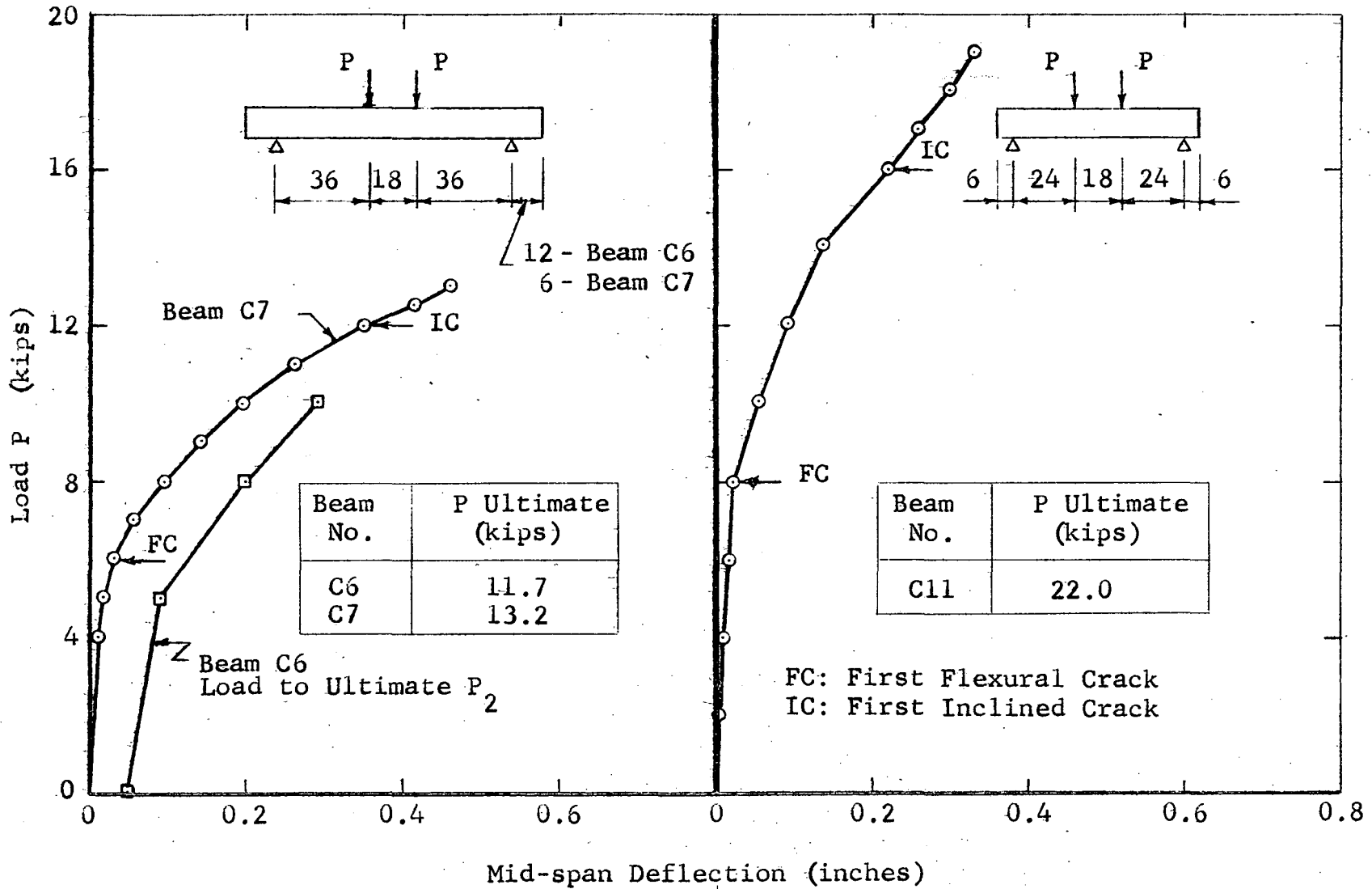


Fig. 16 Load Deflection Curves for Beams C6 and C7 and Beam C11

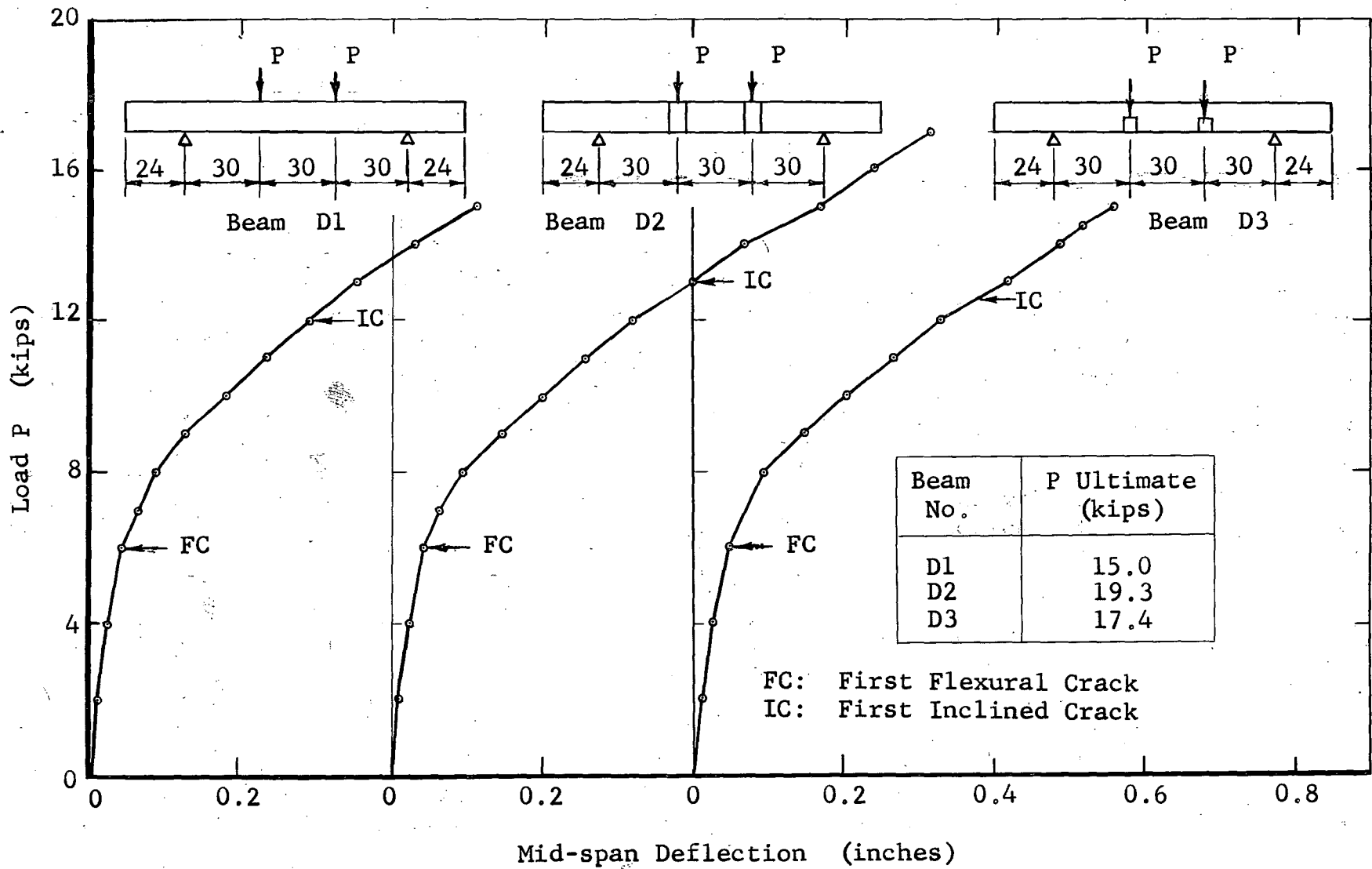


Fig. 17 Load Deflection Curves for Beams D1, D2, and D3



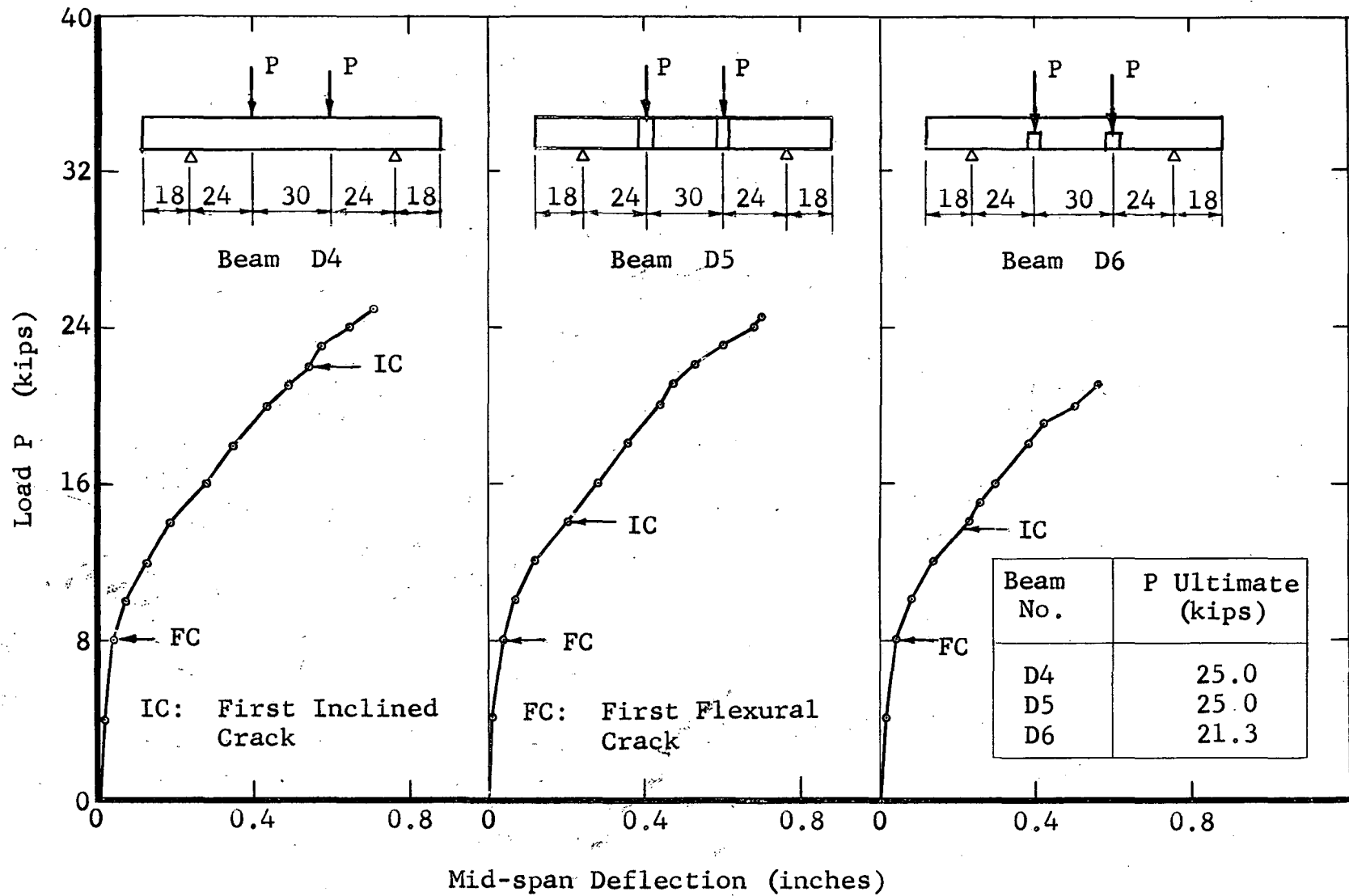


Fig. 18 Load Deflection Curves for Beams D4, D5, and D6

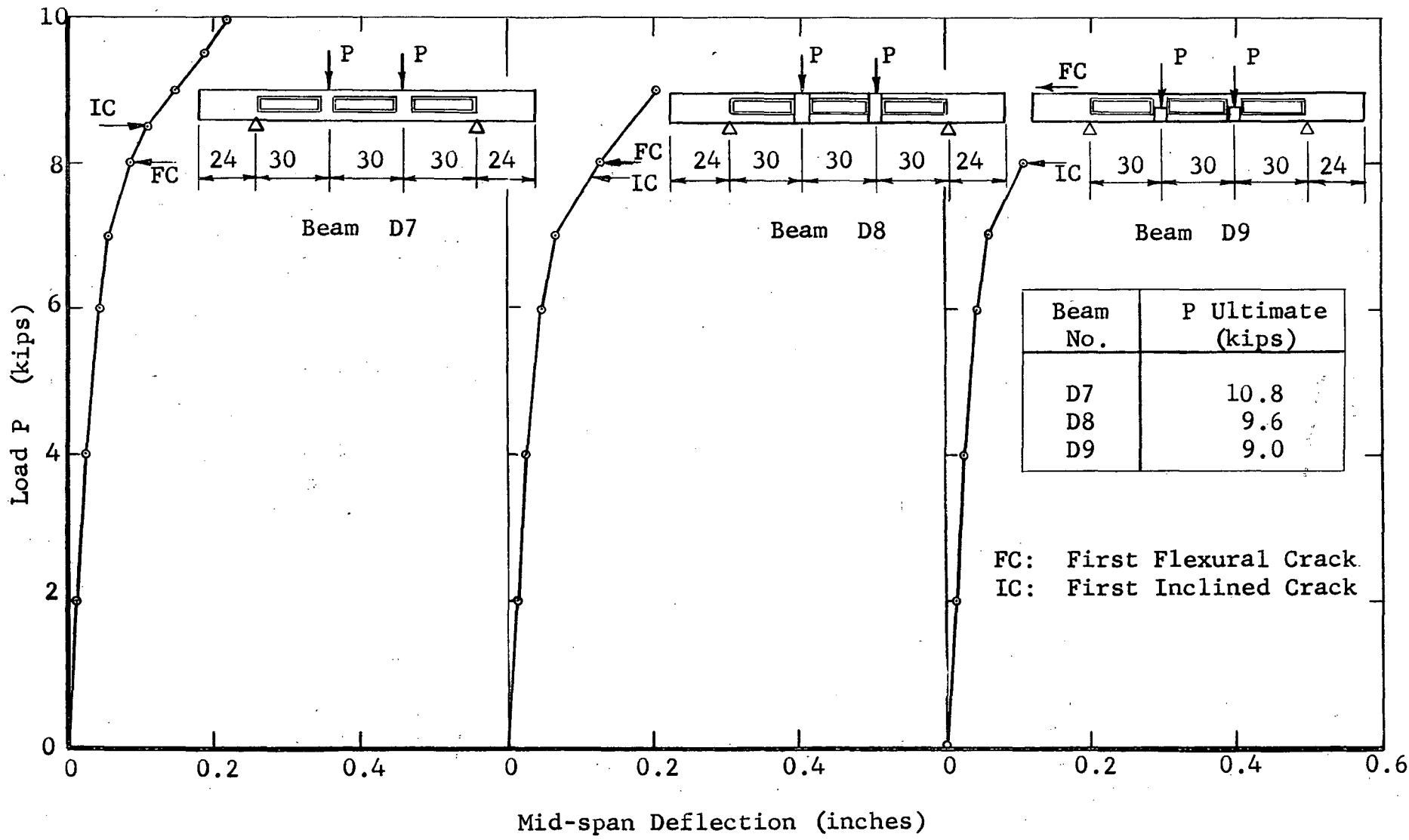


Fig. 19 Load Deflection Curves for Beams D7, D8, and D9

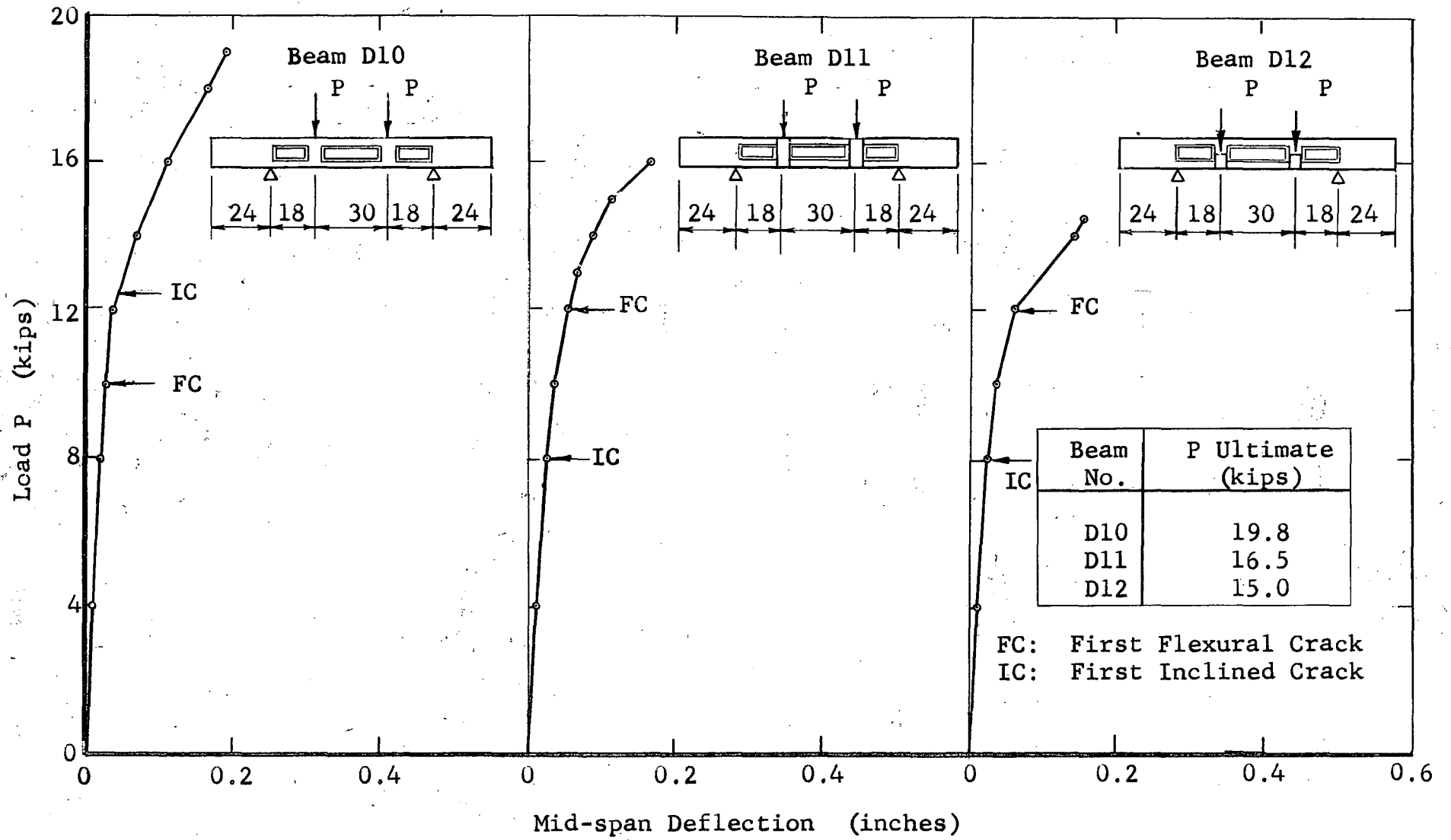
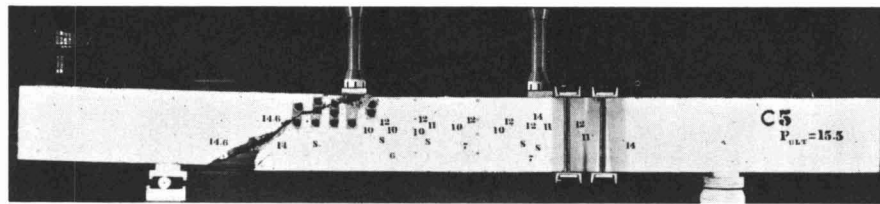
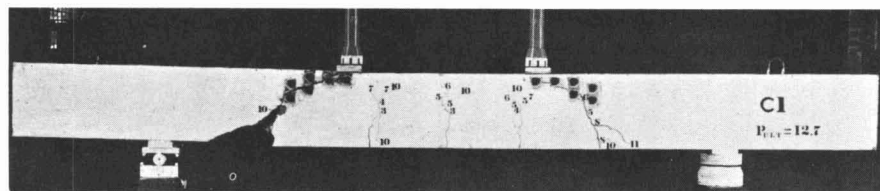


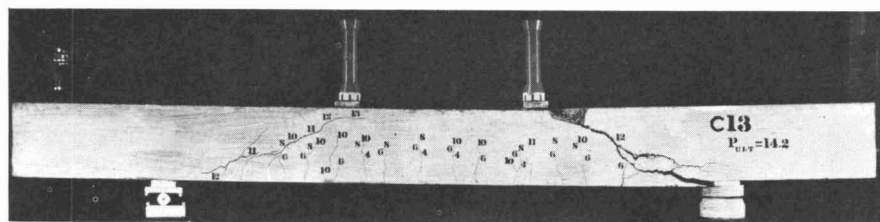
Fig. 20 Load Deflection Curves for Beams D10, D11, and D12



Beam C5 with Prestressed Strands



Beam C1 with Un-prestressed Strands



Beam C13 with Reinforcing Bars

Fig. 21 Beams with 30 in. Shear Span and 24 in. Overhang

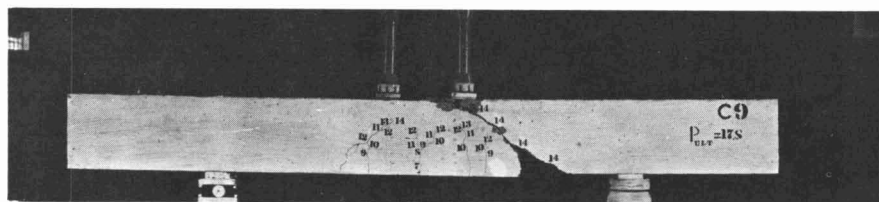
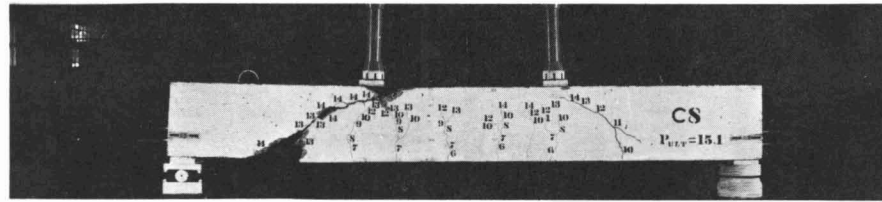
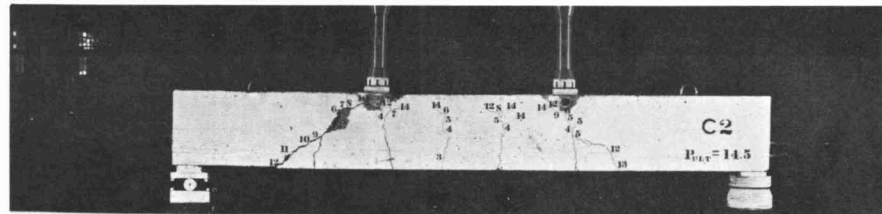


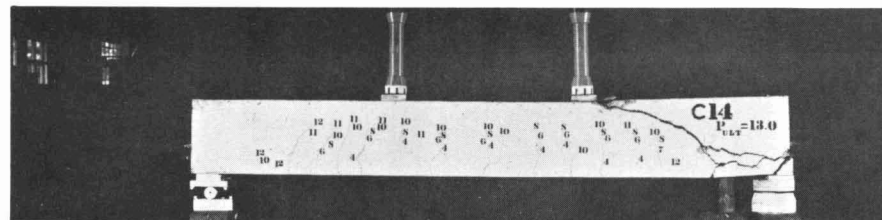
Fig. 22 Beam C9 with 27 in. Shear Span, 24 in. Overhang and Prestressed Strands



Beam C8 with Prestressed Strands



Beam C2 with Un-prestressed Strands



Beam C14 with Reinforcing Bars

Fig. 23 Beams with 30 in. Shear Span and  $2\frac{1}{2}$  in. Overhang

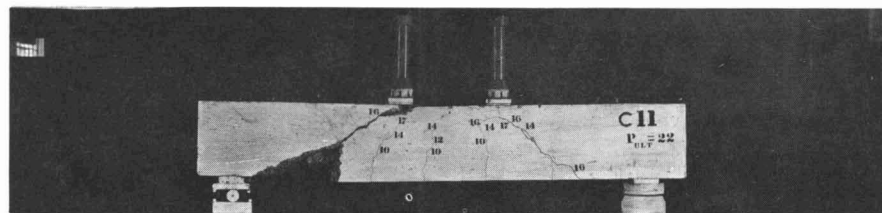
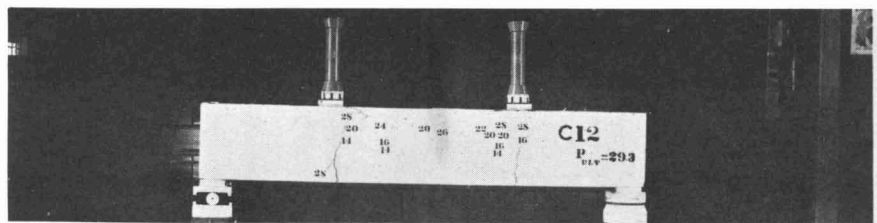
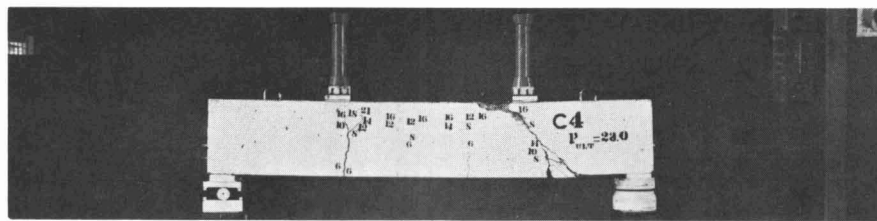


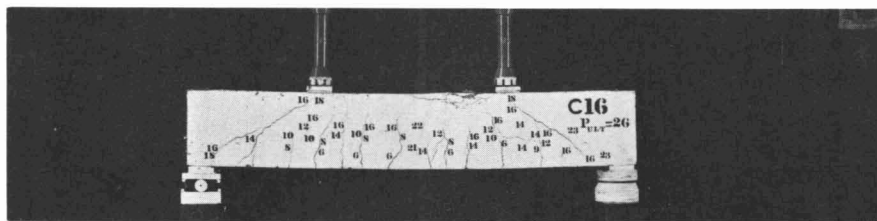
Fig. 24 Beam C11 with 24 in. Shear Span and  $2\frac{1}{2}$  in. Overhang



Beam C12 with Prestressed Strands

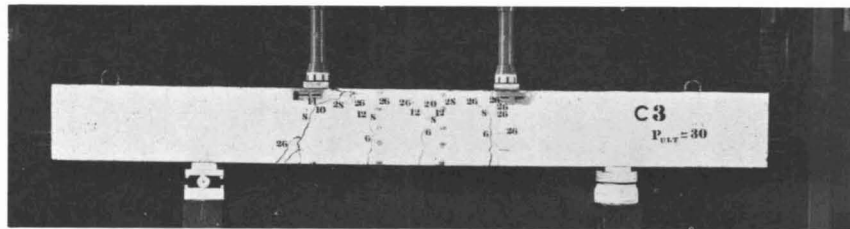


Beam C4 with Un-prestressed Strands

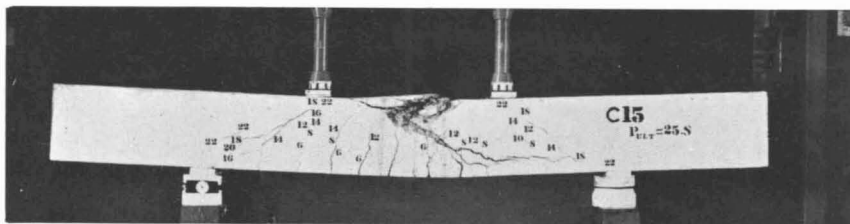


Beam C16 with Reinforcing Bars

Fig. 25 Beams with 18 in. Shear Span and  $2\frac{1}{2}$  in. Overhang

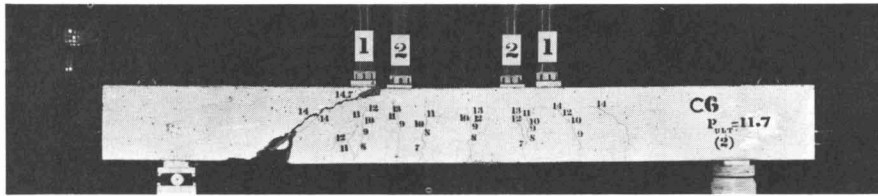


Beam C3 with Un-prestressed Strands

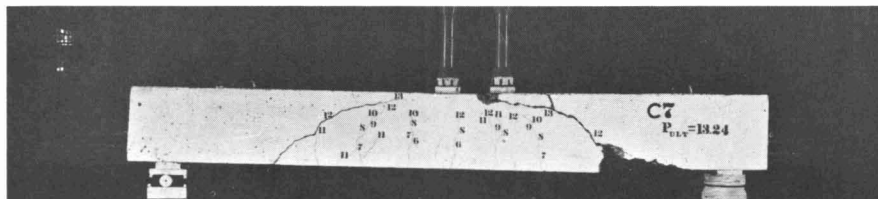


Beam C15 with Reinforcing Bars

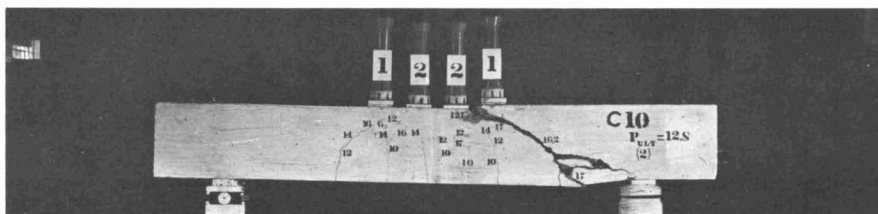
Fig. 26 Beams with 18 in. Shear Span and 24 in. Overhang



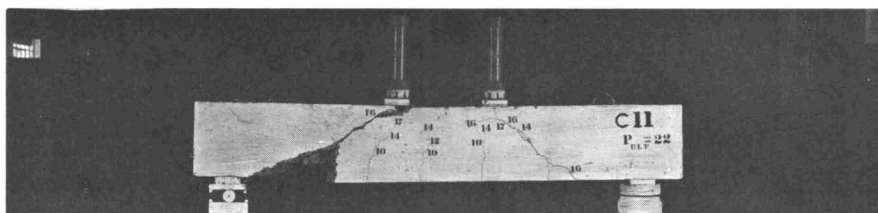
Beam C6 with Initial and Final Shear Spans of 30 and 36 in., Respectively



Comparison Beam C7 having Shear Span of 36 in.



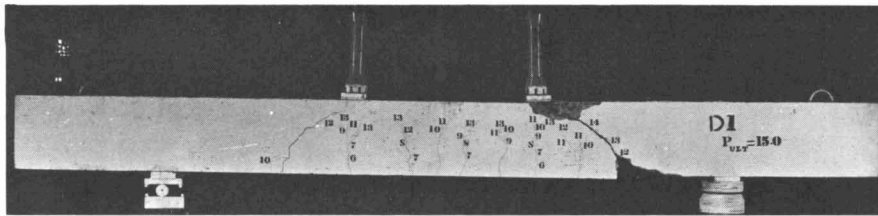
Beam C10 with Initial and Final Shear Spans of 24 and 30 in., Respectively



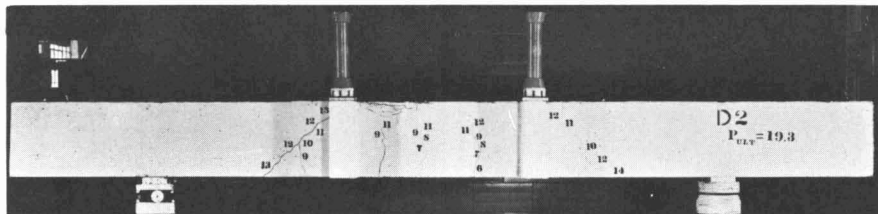
Comparison Beam C11 having Shear Span of 24 in.  
(Note: Comparison Beam C5 is Shown in Fig. 21)

Fig. 27 Reloaded Beams C6 and C10 with Comparison Beams

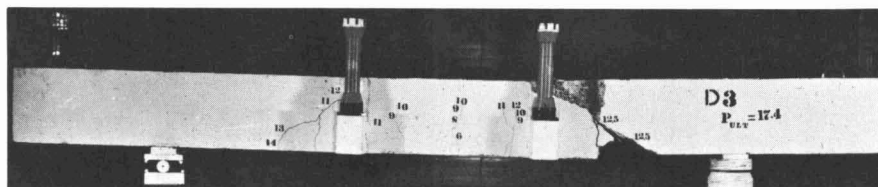




Beam D1 Top Loading

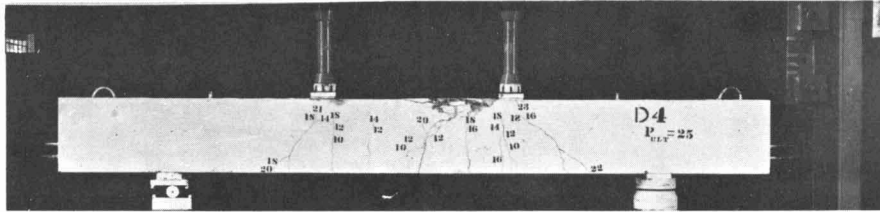


Beam D2 Full Stub Loading

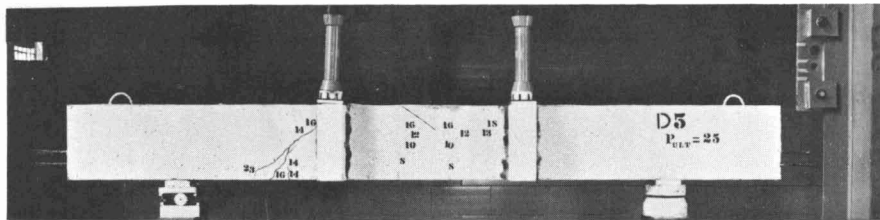


Beam D3 Half Stub Loading

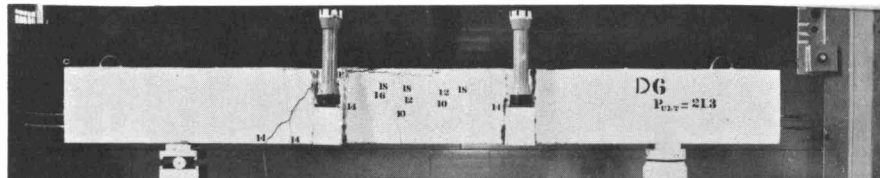
Fig. 28 Rectangular Beams with 30 in. Shear Spans



Beam D4 Top Loading

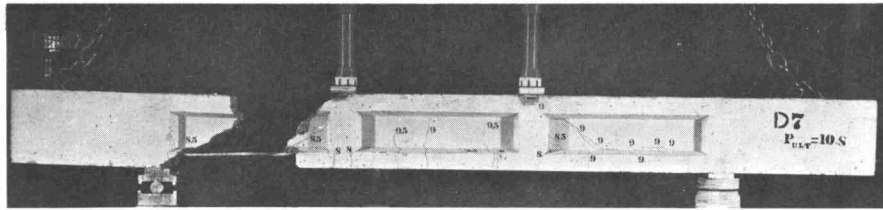


Beam D5 Full Stub Loading

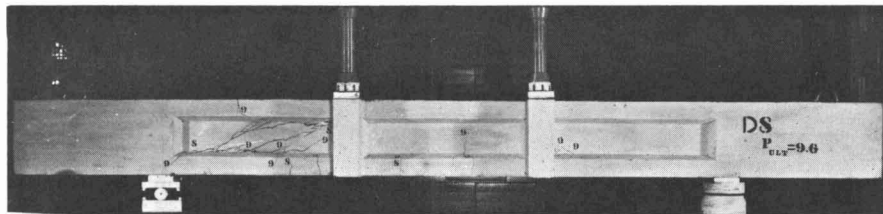


Beam D6 Half Stub Loading

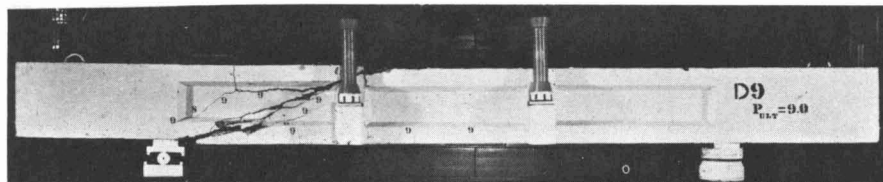
Fig. 29 Rectangular Beams with 24 in. Shear Spans



Beam D7 Top Loading

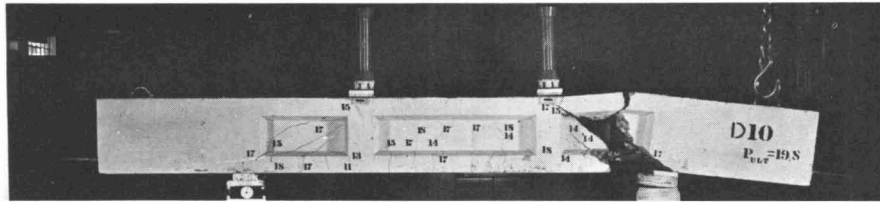


Beam D8 Full Stub Loading

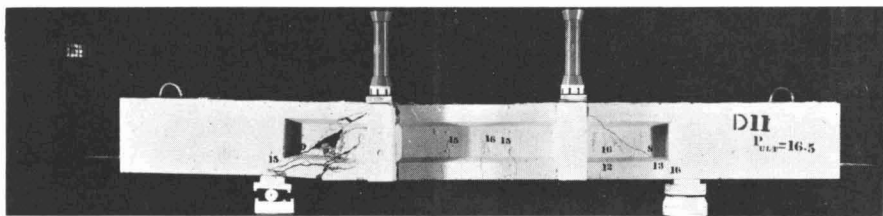


Beam D9 Half Stub Loading

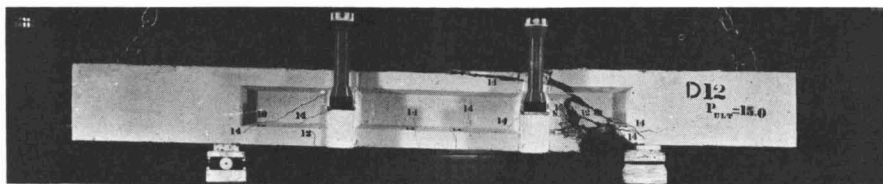
Fig. 30 I-Beams with 30 in. Shear Spans



Beam D10 Top Loading



Beam D11 Full Stub Loading



Beam D12 Half Stub Loading

Fig. 31 I-Beams with 18 in. Shear Spans

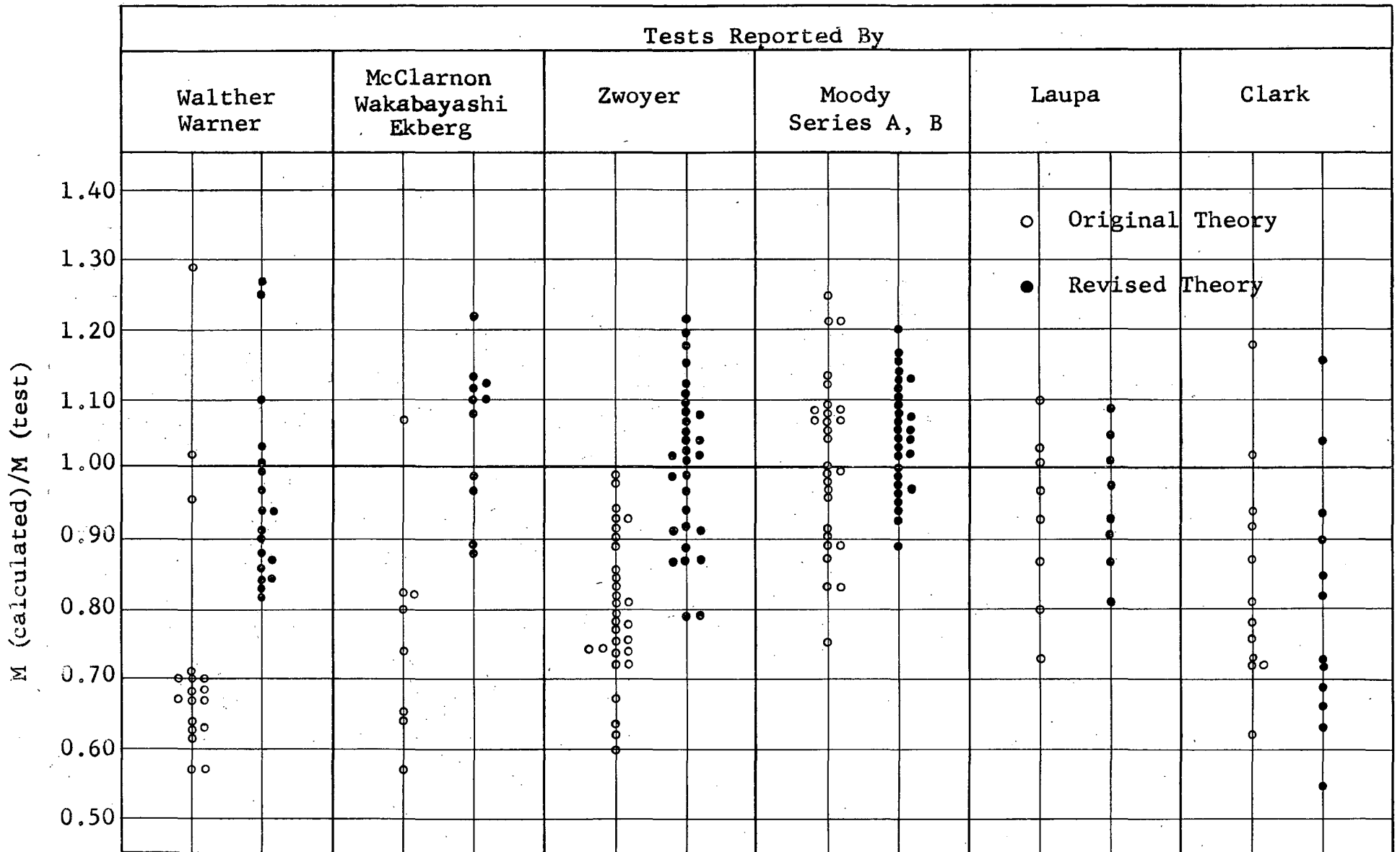
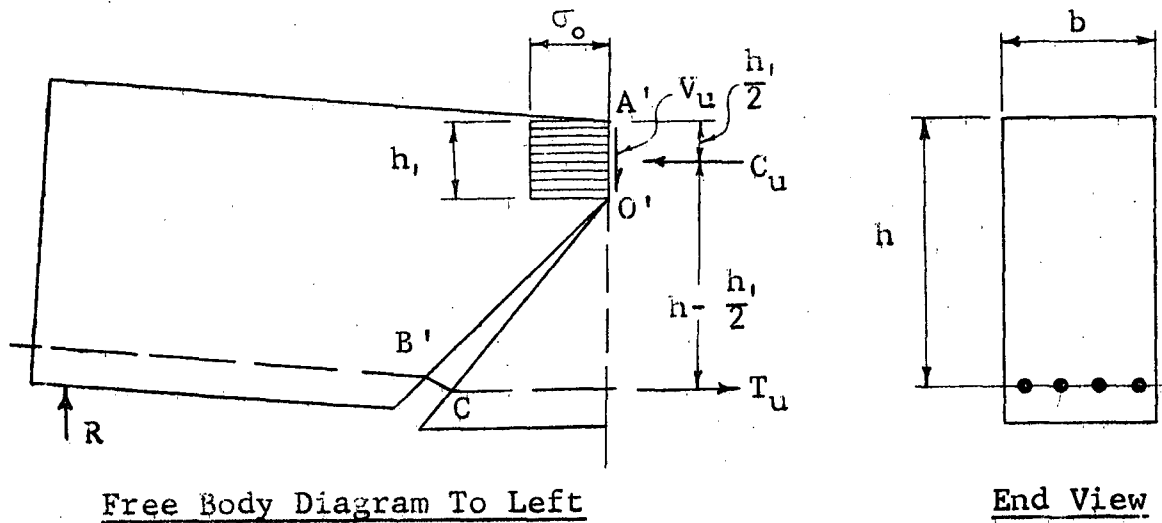
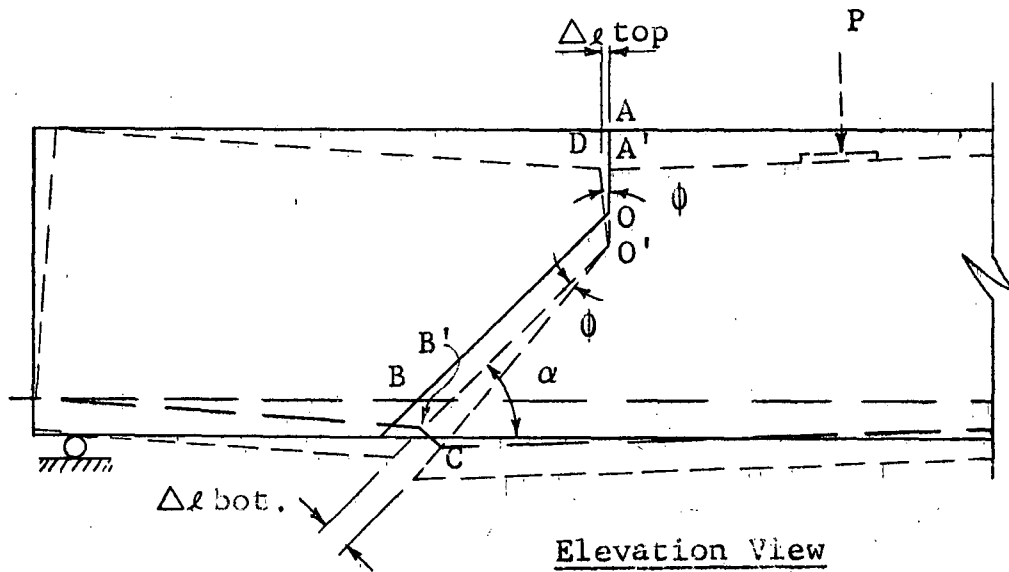


Fig. 32 Comparison of Shear Compression Theory, Original and Revised, with Test Results



Note

1. AO and BO are reference lines at zero load.
2. A'O' and B'O' are displaced reference lines at ultimate load.
3. O'D and O'C define assumed deformations of failure crack,
4.  $\phi = \angle A'O'D = \angle B'O'C$ .
5.  $\alpha$  is angle of inclination of failure crack.
6.  $\Delta l_{top} = A'D$  is deformation of top fiber to the left of A'.
7.  $\Delta l_{bot.} = B'C$  is the crack width at the level of the steel.
8.  $\sigma_o$  is the average compressive stress in the concrete at failure, assumed uniform over the distance  $h_1$ .
9.  $V_u$ ,  $C_u$ , and  $T_u$  are the resultant shear, compressive, and tensile forces acting at the critical section.

Fig. 33 Idealized Mechanism of Failure

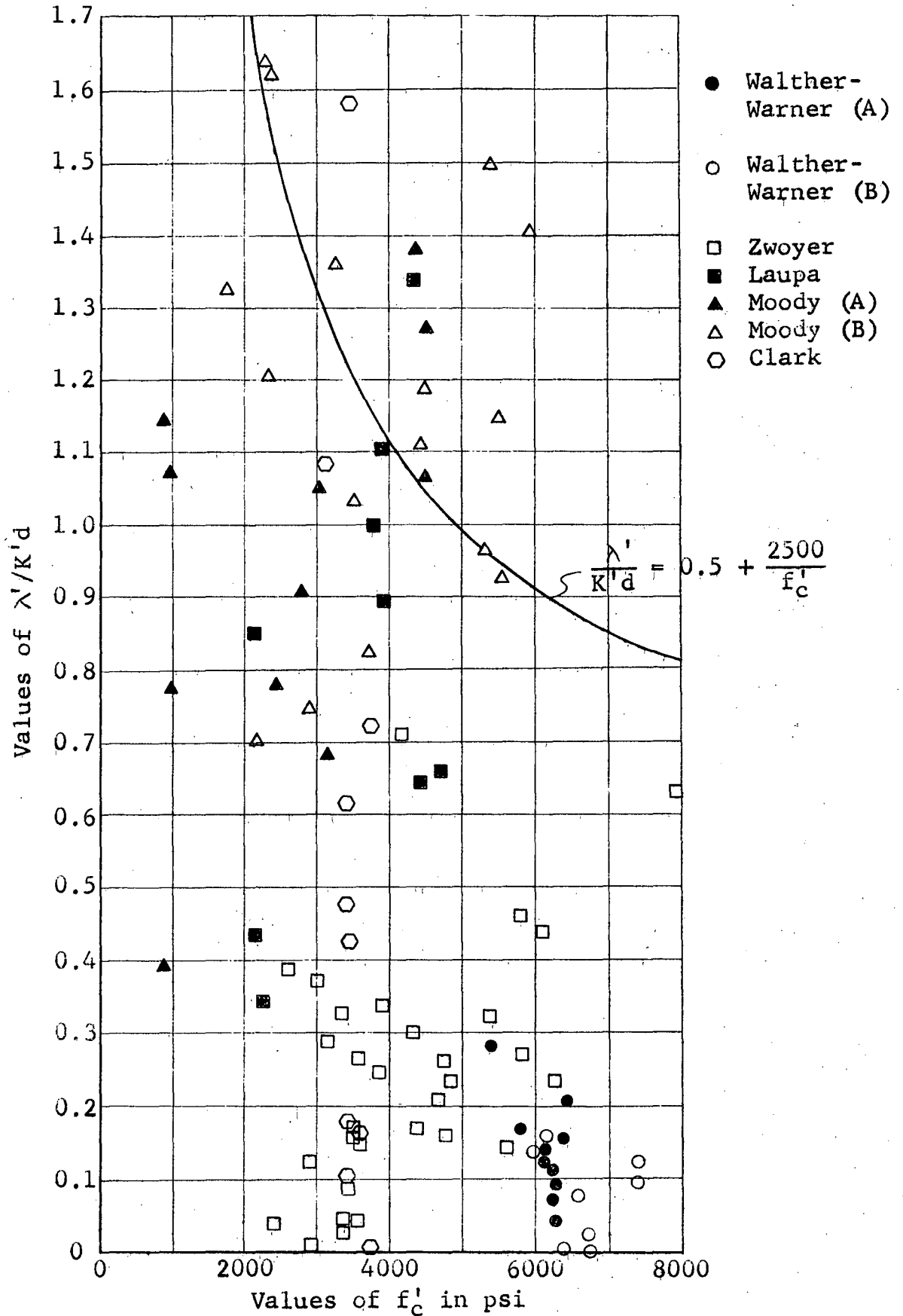


Fig. 34 Relationship between Bond Parameter,  $\lambda'/K'd$ , and  $f'_c$

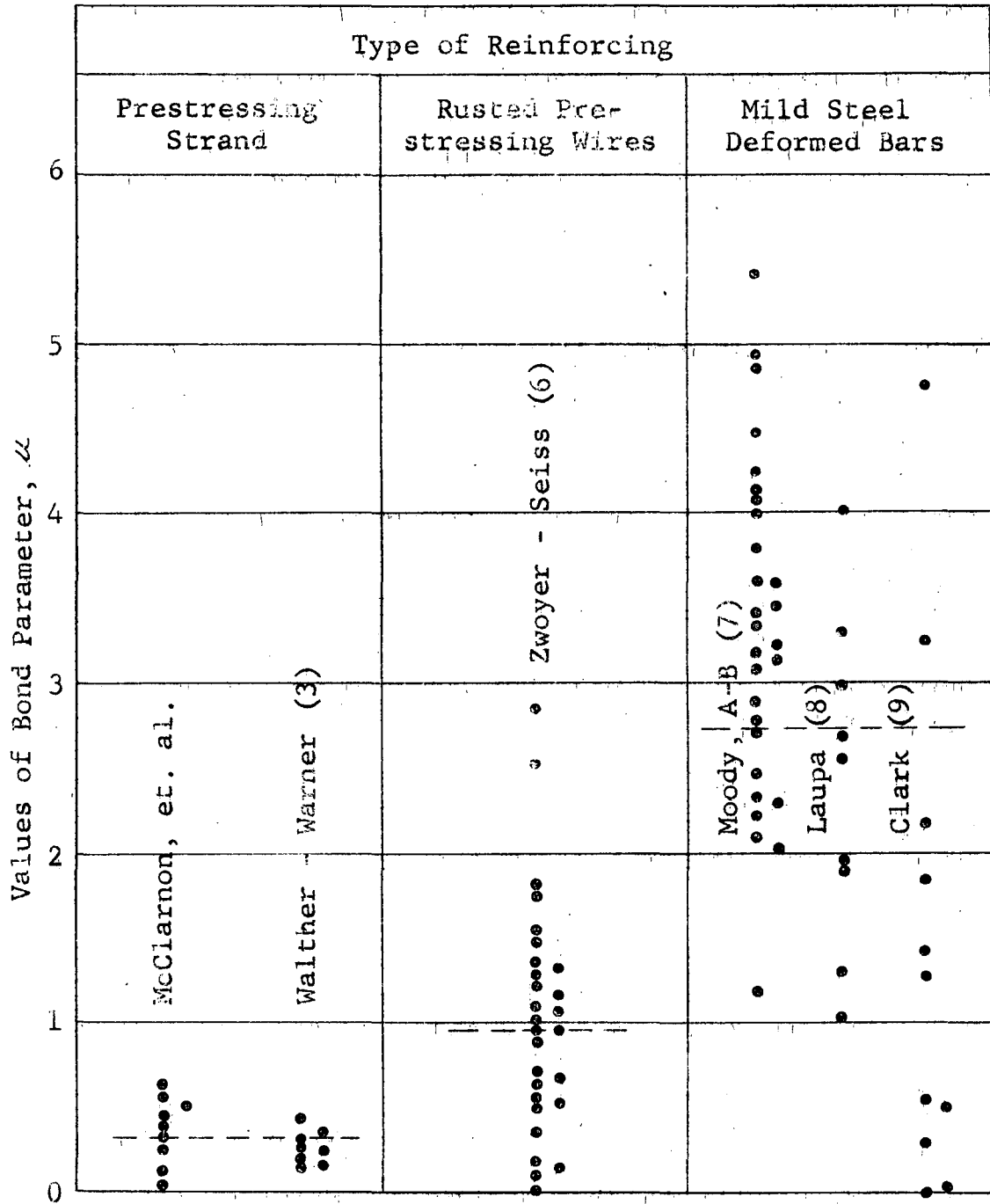


Fig. 35 Relationship Between Bond Parameter Values and Type of Reinforcing



REFERENCES

1. Walther, R.E.  
THE ULTIMATE STRENGTH OF PRESTRESSED AND CONVENTIONALLY REINFORCED CONCRETE UNDER THE COMBINED ACTION OF MOMENT AND SHEAR, Fritz Engineering Laboratory Report No. 223.17, Lehigh University, October 1957.
2. Walther, R.E.  
SHEAR STRENGTH OF PRESTRESSED CONCRETE BEAMS, Fritz Engineering Laboratory Report No. 223.17A, Lehigh University, November 1957.
3. Walther, R.E. and Warner, R.F.  
ULTIMATE STRENGTH TESTS OF PRESTRESSED AND CONVENTIONALLY REINFORCED CONCRETE BEAMS IN COMBINED BENDING AND SHEAR, Fritz Engineering Laboratory Report No. 223.18, Lehigh University, September 1958.
4. ACI-ASCE Joint Committee 323  
TENTATIVE RECOMMENDATIONS FOR PRESTRESSED CONCRETE, Journal of the American Concrete Institute, Vol.29, No. 7, January 1958.
5. Sozen, M.A., Zwoyer, E.M. and Siess, C.P.  
STRENGTH IN SHEAR OF BEAMS WITHOUT WEB REINFORCEMENT, University of Illinois Bulletin No. 452, April 1959.
6. Zwoyer, E.M. and Siess, C.P.  
ULTIMATE STRENGTH IN SHEAR OF SIMPLY SUPPORTED PRESTRESSED CONCRETE BEAMS WITHOUT WEB REINFORCEMENT, Journal of the American Concrete Institute, Vol. 26, No. 2, October 1954.
7. Moody, K.G.; Viest, I.M.; Elstner, R.C.; and Hognestad, E.  
SHEAR STRENGTH OF REINFORCED CONCRETE BEAMS, Journal of the American Concrete Institute, Vol. 26, No. 4 (December 1954), No. 5 (January 1955), No. 6 (February 1955), No. 7 (March 1955).
8. Laupa, A.; Siess, C.P.; and Newmark, N.M.  
STRENGTH IN SHEAR OF REINFORCED CONCRETE BEAMS, University of Illinois Bulletin, Vol. 52, No. 55, March 1955.

9. Clark, A.P.  
DIAGONAL TENSION IN REINFORCED CONCRETE BEAMS,  
Journal of the American Concrete Institute, Vol.  
23, No. 2, October 1951.
10. Billet, D.F.; and Appleton, J.H.  
FLEXURAL STRENGTH OF PRESTRESSED CONCRETE BEAMS,  
Journal of the American Concrete Institute, Vol.  
25, No. 10, June 1954.
11. Ferguson, P.M.  
SOME IMPLICATIONS OF RECENT DIAGONAL TENSION TESTS,  
Journal of the American Concrete Institute, Vol.28,  
No. 2, August 1956.